National Oceanography Centre, Southampton

Research & Consultancy Report No. 11

The airflow distortion at instrument sites on the RRS *James Cook*

B I Moat, M J Yelland & E B Cooper

2006

National Oceanography Centre, Southampton
University of Southampton, Waterfront Campus
European Way
Southampton
Hants SO14 3ZH UK

Author contact details:
Tel: +44 (0)23 8059 7739
Fax: +44 (0)23 8059 6204
Email: bim@noc.soton.ac.uk

DOCUMENT DATA SHEET

AUTHOR

MOAT, B I, YELLAND, M J & COOPER, E B

PUBLICATION DATE

2006

TITLE

The airflow distortion at instrument sites on the RRS *James Cook*.

REFERENCE

Southampton, UK: National Oceanography Centre, Southampton, 44pp.
(National Oceanography Centre Southampton Research and Consultancy Report, No. 11)
(Unpublished manuscript)

ABSTRACT

Wind speed and air-sea flux measurements made from instrumentation on ships are affected by the airflow distortion created by the presence of the ship. The airflow can be either accelerated or decelerated depending on the shape of the ship and the location of the anemometer. The computational fluid dynamics (CFD) package VECTIS was used to examine the extent of the flow distortion at potential anemometer locations on the foremast platform of the RRS *James Cook*. This technique has been previously used to study the airflow over many research ships, but this is believed to be the first time it has been applied to a research ship in the design/build stage.

CFD modelling of the airflow over the ship showed that the foremast platform of the RRS *James Cook* is a good location to locate instrumentation and make high quality air-sea flux measurements. The wind speed is decelerated by about 2 % of the freestream wind speed for bow-on flows at well-exposed anemometer sites on the foremast platform. For relative wind directions up to ±30° of the bow the airflow is accelerated by up to 5 %.

The ship's anemometers are located on the main mast and are relatively close to the ship's large satellite communication radome. For winds within 15° of the bow the wind speeds at these anemometer sites are accelerated by up to about 7 %. For wind directions at ±30° the satellite radome has a significant effect on the flow and the wind speeds will be severely biased, with the magnitude of the bias varying rapidly with wind direction and the angle of pitch of the ship. It is strongly recommended that these anemometers be moved higher up and further away from the mast.

KEYWORDS

Airflow distortion, CFD, computational fluid dynamics, wind speed measurement, RRS James Cook

ISSUING ORGANISATION

National Oceanography Centre, Southampton
University of Southampton, Waterfront Campus
European Way
Southampton SO14 3ZH
UK

THE AIRFLOW DISTORTION AT INSTRUMENT SITES ON THE RRS JAMES COOK

THE AIRFLOW DISTORTION AT INSTRUMENT SITES ON THE RRS JAMES COOK

B. I. Moat, M. J. Yelland and E. B. Cooper

June 2006

1. INTRODUCTION

Wind speed measurements from ship-based anemometers are biased by the distortion of the airflow by the ship's hull and superstructure. For example, previous computational fluid dynamics (CFD) modelling has shown that anemometers located on the foremast platform of the RRS *Charles Darwin* experience a flow distortion of up to 14 % of the freestream or undisturbed wind speed for flows directly over the bow (Yelland et al. 1998). The effect is less severe for wind speed measurements made from the foremast platform of the RRS *Discovery* as the ship is more streamlined in shape (Yelland et al. 2002). The Natural Environment Research Council (NERC) is to take delivery of its latest research ship, the RRS *James Cook,* in September 2006. This ship will be a replacement for the RRS *Charles Darwin*. To obtain high quality wind speed and air-sea flux measurements from the RRS *James Cook* the effect of flow distortion has to be taken into account. This report documents the results of the CFD modelling of the ship at three relative wind directions and the best locations for positioning anemometers are presented.

In general, the effects of flow distortion can be minimised for winds forwards of the beam by locating anemometers in well-exposed locations as high as possible above foremast platforms (Moat et al. 2006). In addition, the position and shape of a ship's superstructure will influence the amount that the airflow is distorted above the front deck (Moat et al. 2005), i.e. an abrupt block-like superstructure located close to the foremast in the bows of the ship can significantly affect the wind speed measurements made from anemometers located on the foremast platform. Therefore during the specification stage of the RRS *James Cook* it was stated that the superstructure must be streamlined in shape, i.e. "layered and raked towards the aft, not an abrupt high bridge front".

The CFD software VECTIS (Ricardo, 2005) was used to simulate the flow of air over the RRS *James Cook* and the absolute wind speed errors at a number of

anemometer locations were estimated. The VECTIS code is described in Section 2 and the anemometer positions above the foremast and main mast are detailed in Section 3. The effects of flow distortion are dependent on the anemometer location and vary with changes in relative wind direction (Yelland et al., 2002). Therefore the airflow over the ship was simulated for flows directly over the bow, flows 15° off the port bow and flows 30° off the port bow. Effective anemometer positions were created to enable the wind speed bias for winds at 15° and 30° off the starboard bow to be calculated from the two VECTIS simulations of the airflow over the port bow. Further information on this technique is included in Moat and Yelland (1997). The CFD results at these relative wind directions are presented in Section 4. The variation in wind speed error with height above the foremast platform is discussed in Section 5.

2. DESCRIPTION OF THE CFD MODELLING

VECTIS is a commercial three-dimensional Reynolds Averaged Navier-Stokes solver, which has been used successfully since 1994 to model the airflow over many research ships (Yelland et al. 1998; 2002). The VECTIS models only reproduce the steady state mean flow characteristics, and do not simulate the turbulence structure. The standard $k \sim \varepsilon$ (Launder and Spalding, 1972) turbulence closure model was used to parameterise the turbulence. Except when the anemometer is in the wake of an upstream obstacle, VECTIS simulations of the airflow over detailed ship models are accurate to within 2 % (Yelland et al. 2002) for well-exposed anemometer locations on research ships.

A numerical representation of the full-scale 3-dimensional ship geometry was provided by Skipsteknisk AS, Naval Architects, Norway. Over a period of 3 weeks the software package FEMGEN (Femsys 1992) was used to convert the supplied geometry into the format required by the VECTIS software. The numerical representation of the geometry was very detailed (Figure 1) and reproduced the actual geometry to within 0.1 m. The general ship dimensions are 89.5 m in overall length and 18.6 m in breadth. A computational domain was defined around the geometry with the ship in the centre. The width of the domain increased with the ship's orientation to the flow to prevent spurious increases in wind speed created by the blockage of the ship in the domain. For flows directly

over the bow (head to wind) the domain size was 600 m in length, 600 m wide and 200 m high. For flows at relative wind directions of 15° and 30° off the bow the domain width increased to 700 m and 1000 m respectively. In general, the ratio of the frontal area of the ship to the area of the inlet gave a blockage by the ship of less than 1 %.

The number of computational cells within the domain increased from 1.9 million for the flow directly over the bow to 3.2 million at a relative wind direction of 30°. The time taken for the solutions to converge was 5-7 days using a 2.4 GHz Opteron processor on a Linux workstation. This fast convergence time was obtained using the steady-state rather than the time-marching solver (Moat and Yelland 2006). The cell sizes varied throughout the computational domain with high-resolution cells in the vicinity of the foremast (cells of 0.13 m) and much lower resolution cells in areas well away from the ship where the flow did not vary very rapidly.

The vertical profile of the velocity at the domain inlet was specified as a fully logarithmic boundary layer profile with a wind speed at a height of 10 m of 15 ms^{-1}. The domain floor was allocated a small roughness length (order 10^{-4} m) in order to maintain the profile downwind of the inlet. All results presented in this report were obtained by comparing the wind speed at a particular anemometer position with the freestream wind speed profile well abeam (more than 100 m) of the anemometer position to arrive at a percentage wind speed bias for that position.

3. EXAMPLE ANEMOMETER POSITIONS

The exact location of any permanently installed anemometers on the foremast is not yet decided. For the purpose of this study five well-exposed example anemometer positions above the foremast platform were selected to illustrate the effects of the airflow distortion in this region. These corresponded to three anemometer sites on the front edge of the platform and two located at the port and starboard extremes (Figure 2a) of the platform. Anemometer heights of 2.8 m above the foremast platform were selected, as this is the typical height of anemometers used in recent air-sea flux studies using instruments mounted

temporarily on the foremast of the RRS *Discovery*. The airflow distortion at other anemometer heights is discussed in Section 5. Table 1 details the instrument positions in the VECTIS co-ordinate system (where the origin is at the centre of the ship at sea level) for the three wind directions modelled. Table 1 also includes the known positions of the two ship's anemometers located on a mast above the ship's bridge (Figure 2b).

The effective anemometer positions for the airflow over the starboard bow are not listed in Table 1. This is because the ship geometry is symmetrical which means the wind speed error at effective anemometer positions for flows over the starboard bow can be calculated from those simulations over the port bow. For example, the wind speed error at the 'S2' location for a flow over the port bow will be the wind speed error at the 'P2' location for flow over the starboard bow. See Moat and Yelland, (1997) for more detail.

	Anemometer	X, along (m)	Y, across (m)	Z, above (m)
0° (head to wind)	P2	43.40	2.02	19.91
	P1	44.47	0.74	19.91
	C	44.47	0	19.91
	S1	44.47	-0.74	19.91
	S2	43.40	-2.02	19.91
	port ship	-1.03	0.57	31.61
	starboard ship	-1.03	-0.57	31.61
-15° (port airflow)	P2	42.44	-9.28	19.91
	P1	43.15	-10.77	19.91
	C	42.96	-11.51	19.91
	S1	42.76	-12.22	19.91
	S2	41.40	-13.18	19.91
	port ship	-0.85	0.82	31.61
	starboard ship	-1.14	-0.28	31.61
-30° (port airflow)	P2	38.60	-19.95	19.91
	P1	38.88	-21.59	19.91
	C	38.51	-22.24	19.91
	S1	38.14	-22.88	19.91
	S2	36.58	-23.45	19.91
	port ship	-0.61	1.00	31.61
	starboard ship	-1.18	0.02	31.61

Table 1 Anemometers positions in the VECTIS co-ordinate system. The z value is the height of the anemometer above the design waterline of the ship. A schematic of the locations are shown in Figures 2a) and b).

4. CFD RESULTS

4.1 Introduction

The following section contains the CFD estimates of the absolute wind speed errors for the three relative wind directions modelled. The freestream wind speeds were extracted towards the edge of the tunnel at the anemometer height. The freestream flow has small, predictable gradients and can be estimated accurately at any given point on the vertical profile. In contrast, the flow at the instrument site can suffer from server distortion and large gradients in the velocity field. Additionally it is not always possible to define the mesh so that the instruments are at the exact centers of the computational cells (see Moat et al., 1996). Therefore the velocity at an instrument site was obtained from an average of three values estimated from lines of data extracted in three directions. The percentage wind speed error is given by:

$$\%Error = \left(\frac{Average\ velocity}{Free\ stream\ velocity} - 1 \right) \times 100 \qquad (1)$$

with a positive error indicating an acceleration of the flow.

For each relative wind direction the percentage wind speed errors on a horizontal plane at the height of the anemometers are shown in Figures 3 to 5. The wind speed errors at the various anemometer positions are contained in Sections 4.2 to 4.4 and are discussed in Section 4.5.

4.2 The wind speed error for flows directly over the bow (0 degrees)

For bow-on winds the flow is symmetric about the ship's centerline, hence only lines of velocity data through the P2, P1, C and port ship's anemometer locations are shown in Figures 6 to 9. The percentage wind speed errors for all anemometer sites are summarized in Table 2. A positive error indicates an acceleration of the flow.

anemometer	Velocity from each direction (ms^{-1})	Average velocity at anemometer site (ms^{-1})	freestream wind speed (ms^{-1})	% error
P2	15.724 (x) 15.728 (y) 15.729 (z)	15.727	15.955	-1.43
P1	15.689 (x) 15.688 (y) 15.689 (z)	15.689	15.954	-1.66
C	15.705 (x) 15.704 (y) 15.705 (z)	15.705	15.954	-1.56
S1	15.689 (x) 15.688 (y) 15.689 (z)	15.689	15.954	-1.66
S2	15.724 (x) 15.728 (y) 15.729 (z)	15.727	15.955	-1.43
Ship port	17.791(x) 17.795 (y) 17.792 (z)	17.793	16.663	6.78
Ship starboard	17.791(x) 17.795 (y) 17.792 (z)	17.793	16.663	6.78

Table 2 The absolute wind speed errors for a wind direction of 0° (head to wind).

4.3 The wind speed error for flows ±15 degrees off the bow

Figures 10 to 16 show the lines of velocity data through the five foremast and two mainmast anemometer locations for a wind at 15° off the bow. The results for all anemometer sites are summarized in Table 3. 5.

anemometer	Velocity from each direction (ms^{-1})	Average velocity at anemometer site (ms^{-1})	Freestream wind speed (ms^{-1})	% error
P2	15.770 (x) 15.770 (y) 15.770 (z)	15.770	15.950	-1.13
P1	15.823 (x) 15.822 (y) 15.822 (z)	15.822	15.950	-0.80
C	15.911 (x) 15.911 (y) 15.911 (z)	15.911	15.948	-0.23
S1	15.961 (x) 15.967 (y) 15.968 (z)	15.965	15.949	0.10
S2	16.072 (x) 16.072 (y) 16.071 (z)	16.072	15.950	0.76
ship port	17.765 (x) 17.773 (y) 17.768 (z)	17.768	16.660	6.65
ship starboard	17.790 (x) 17.782 (y) 17.797 (z)	17.790	16.660	6.78

Table 3 The absolute wind speed errors for a wind direction at 15° off the port bow.

4.4 The wind speed error for flows ±30 degrees off the bow

Figures 17 to 23 show the lines of velocity data through all the anemometer locations for winds at 30° off the bow. The results for all anemometers are summarized in Table 4.

anemometer	Velocity from each direction (ms^{-1})	Average velocity at anemometer site (ms^{-1})	Freestream wind speed (ms^{-1})	% error
P2	16.240 (x) 16.240 (y) 16.241 (z)	16.240	15.949	1.82
P1	16.348 (x) 16.348 (y) 16.348 (z)	16.348	15.946	2.52
C	16.463 (x) 16.462 (y) 16.463 (z)	16.463	15.948	3.23
S1	16.538 (x) 16.538 (y) 16.538 (z)	16.538	15.947	3.71
S2	16.684 (x) 16.684 (y) 16.684 (z)	16.684	15.947	4.62
ship port	16.636 (x) 17.962 (y) 18.447 (z)	17.682	16.656	6.16
ship starboard	20.157 (x) 19.445 (y) 20.671 (z)	20.091	16.656	20.62

Table 4 The absolute wind speed errors for a wind direction at 30° off the port bow.

4.5 Discussion

4.5.1 Example foremast locations

The anemometers located on the foremast are all in well-exposed positions for airflows between ±30° off the bow and have a reasonably low wind speed error (summarised in Table 5). The airflow distortion varies from under estimates of 2 % of the freestream airflow (for bow on flows) to over estimates of 5 % for airflows at 30° over the bow. It can be seen from Figures 6 to 8, 10 to 14 and 17 to 21 that the rate of change of velocity is small, order 1 % per metre. This, and the high resolution provided by the dense mesh gives confidence that the results are accurate, possibly to within the 2 % accuracy shown by Yelland et al. (2002).

The front edge of the foremast platform has the better exposure (P1, C and S1 in Figure 2) and is recommended for fast sampling anemometers and other instrumentation required to directly measure the air-sea fluxes of momentum, heat and moisture. The flow distortion at the other two anemometer locations (P2 and

S2) is sufficiently low to be used to site anemometers for measurements of the mean wind speed.

4.5.2 Ship's anemometers on the main mast

For wind directions of 0° and ±15° the wind speed error for the ship's anemometers is about 7 %. However, it can be seen from Figures 9, 15 and 16 that the anemometers are mounted only 2 m above the region which is severely affected by the wake from the satellite communication radome. When the ship pitches this wake may impinge on the anemometers.

The wind speed bias for 30° flows is given in Table 4 as 6 and 21 % for the upwind and downwind anemometers respectively. However, it can be seen from Figures 22 and 23 that the spatial rate of change of velocity is up to about 4 ms^{-1} per metre (i.e. about 20 % bias per meter), due to a) the influence of the upwind satellite radome (See Figure A4 in the Appendix), b) the proximity of the anemometers to the main mast itself, and c) the coarse mesh density (about 1 m) used in this area of the model. In reality, variations of wind direction or ship's pitching angle mean that the biases cannot be reliably estimated, even if the model was to be repeated with a much tighter mesh around the main mast. If reliable data is required from the ship's anemometers (for example if the wind speed data is used for dynamic ship positioning, or for synoptic meteorological observations reported to the World Meteorological Organisation by the ship's officers) then the ship's anemometers should be moved much higher up the main mast, and preferably further away from the mast itself. More work would be needed to determine a suitable location, but a rough guide is that an anemometer should be more than 3 obstacle diameters away from the obstacle in order to reduce biases to 5 % or less (Gill et al., 1967). The mast diameter is 0.2 m and the satellite radome is about 4.5 m in diameter. Figure 23c suggests that the height should be increased by at least 4 m (to a distance of 2 radome diameters) to a position where at least the rate of change of the bias is lessened.

anemometer		Absolute wind speed error (%) for relative wind directions					
	Location	Height (m)	-30°	-15°	0°	15°	30°
P2	foremast	19.91	2	-1	-1	1	5
P1	foremast	19.91	3	-1	-2	0	4
C	foremast	19.91	3	0	-2	0	3
S1	foremast	19.91	4	0	-2	-1	3
S2	foremast	19.91	5	1	-1	-1	2
Port ship	Main mast	31.61	-	7	7	7	-
Starboard ship	Main mast	31.61	-	7	7	7	-

Table 5 The absolute wind speed error (% of the freestream wind speed) found from the CFD models are given for 5 relative wind directions. A wind direction of 0° indicates a bow-on flow, and a negative direction indicates a flow over the port bow. A negative wind speed error indicates the flow has been decelerated. Values of '-' indicate regions where the error cannot be estimated reliably.

5. THE VARIATION IN WIND SPEED ERROR WITH ANEMOMETER HEIGHT

Anemometers should always be located as high as possible above the foremast platform to minimise the flow distortion created by the presence of the platform, but this may not always be practical due to other instrumentation sited on the same foremast. The variation in the wind speed error with height above the foremast platform through the 'C' anemometer location is shown in Figure 24. This is typical of the wind speed profile along the front edge of the platform. Ideally a minimum of 2 m should be used to avoid the high rates of change in velocity close to the top of the platform.

To aid anemometer placement contour plots of the wind speed error at heights of 2 m and 4 m above the foremast platform are shown for airflows directly over the bow in Figure 25, 15° off the port bow in Figure 26 and 15° off the port bow in Figure 27. In all cases is can be seen that the rate of change of the bias with horizontal position is smaller at a height of 4 m than at a height of 2 m.

6. SUMMARY

The airflow over the RRS *James Cook* has been modeled using the CFD code VECTIS. The airflow distortion at five example anemometer locations on the foremast platform has been quantified for a wind speed of 15 ms^{-1} blowing at five relative wind directions. These ranged from ±30°, ±15° and a flow directly over the bow (0°). The distortion to the airflow was only that created by the ship's hull and superstructure, since small-scale obstructions (the railings and thin masts) cannot be modelled. The wind speed errors for all the instruments are summarised in Table 5.

The foremast platform is a good location to site anemometers on the RRS *James Cook*. For relative wind directions between ±30° of the bow the airflow distortion varies from under estimates of 2 % of the freestream wind speed (for bow on flows) to over estimates of 5 % for airflows at 30° over the bow. However, it is recommend that mean meteorological sensors be placed at the extremes of the foremast platform (P2 and S2 – Figure 2), leaving the forward edge of the platform free to give good exposure for fast sampling anemometers and other instrumentation required to directly measure the air-sea fluxes of momentum, heat and moisture.

Ideally, anemometers should be placed as high as possible above the foremast platform to minimise the effects of distortion of the airflow by the platform itself. As this is not always practical, a minimum height of 2 m should be used.

For wind directions within 15° of the bow the ship's anemometers show accelerations in wind speed of about 7 % compared to the freestream wind speed, but this value may change with the ship's pitching angle. For wind directions outside this range the ship's anemometers are in a region where flow distortion will be both severe and sensitive to wind direction and ship's pitch. If data from these anemometers is to be relied on in any way, for example incorporated into a dynamic ship positioning system or used for synoptic meteorological observations reported to the World Meteorological Organisation, then it is strongly recommended that these instruments are re-located higher up, and preferably further from, the mast.

ACKNOWLEDGEMENTS

We are grateful to Jan Erik Ludviksen of Skipsteknisk AS, Naval Architects, Norway for providing the three dimensional numerical representation of the RRS *James Cook* geometry. The research was funded by the National Oceanography Centre (UK) Technology Innovation Fund.

REFERENCES

Femsys, 1992: FEMGV User Manual, Femsys Ltd., Leicester, United Kingdom, 598 pp.

Gill, G. C., L. E. Olsson, J. S. Sela and M. Suda, 1967: Accuracy of wind measurements on towers and stacks, *Bulletin of the American Meteorological Society*, **48**, 665-674.

Launder, B. E. and D. B. Spalding, 1974: The numerical computation of turbulent flows, *Computer Methods in Applied Mechanics and Engineering*, 3, 269 – 289.

Moat,B. I., Yelland, M. J. and Hutchings, J. 1996: Airflow over the RRS Discovery using the Computational Fluid Dynamics package VECTIS, *SOC Internal Document No. 2,* Southampton Oceanography Centre, Southampton. UK. 41pp. [available from the National Oceanography Centre, Southampton, UK.]

Moat, B. I. and M. J. Yelland, 1997: Airflow 15 and 30 degrees off the bow of the R.R.S. Discovery: the disturbance of the flow at the anemometer sites for cruises D199-D201 and D213-D214, *SOC Internal Document No. 25*, Southampton Oceanography Centre, Southampton. UK. 44pp. [available from the National Oceanography Centre, Southampton, UK.]

Moat, B. I., M. J. Yelland, A. F. Molland and R. W. Pascal, 2005: The effect of ship shape and anemometer location on wind speed measurements obtained from ships, *Proceedings of the 4th International Conference on Marine Hydrodynamics (Marine CFD 2005),* March 30 - 31, University of Southampton, UK, 133-139. [Available from the Royal Institution of Naval Architects, London, UK.]

Moat, B. I. and M. J. Yelland, 2006: Validation of the VECTIS steady-state solver. In prep for NOC Internal Document. National Oceanography Centre, UK.

Moat, B. I., M. J. Yelland and A. F. Molland, 2006: Quantifying the airflow distortion over merchant ships: Part II: application of the model results. *Journal of Atmospheric and Oceanic Technology,* **23**(3), 351-360.

Ricardo, 2005: VECTIS Computational Fluid Dynamics (Release 3.9) user manual, Ricardo Consulting Engineers Ltd., Shoreham-by-Sea, UK, 578 pp.

Yelland, M. J., B. I. Moat, P. K. Taylor, R. W. Pascal, J. Hutchings and V. C. Cornell, 1998: Wind stress measurements from the open ocean corrected for airflow distortion by the ship, *Journal of Physical Oceanography*, **28**(7), 1511-1526.

Yelland, M. J., B. I. Moat, R. W. Pascal and D. I. Berry, 2002: CFD model estimates of the airflow over research ships and the impact on momentum flux measurements, *Journal of Atmospheric and Oceanic Technology,* **19**(10), 1477-1499.

FIGURES

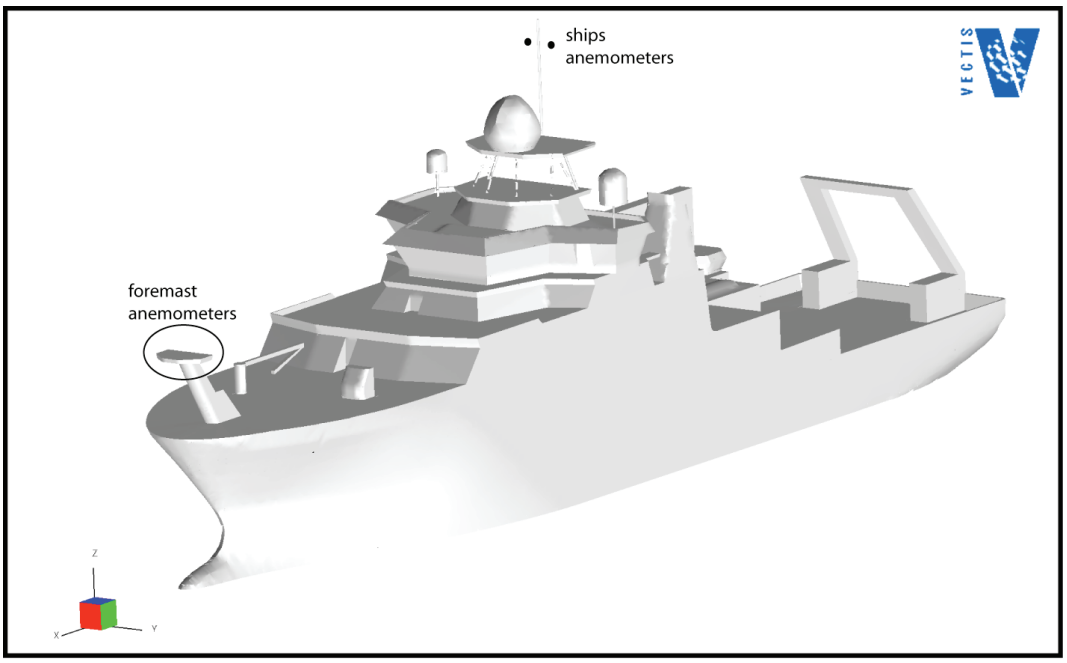

Figure 1 Numerical representation of the RRS *James Cook* geometry. The foremast instrument location and the ship's anemometer positions are indicated.

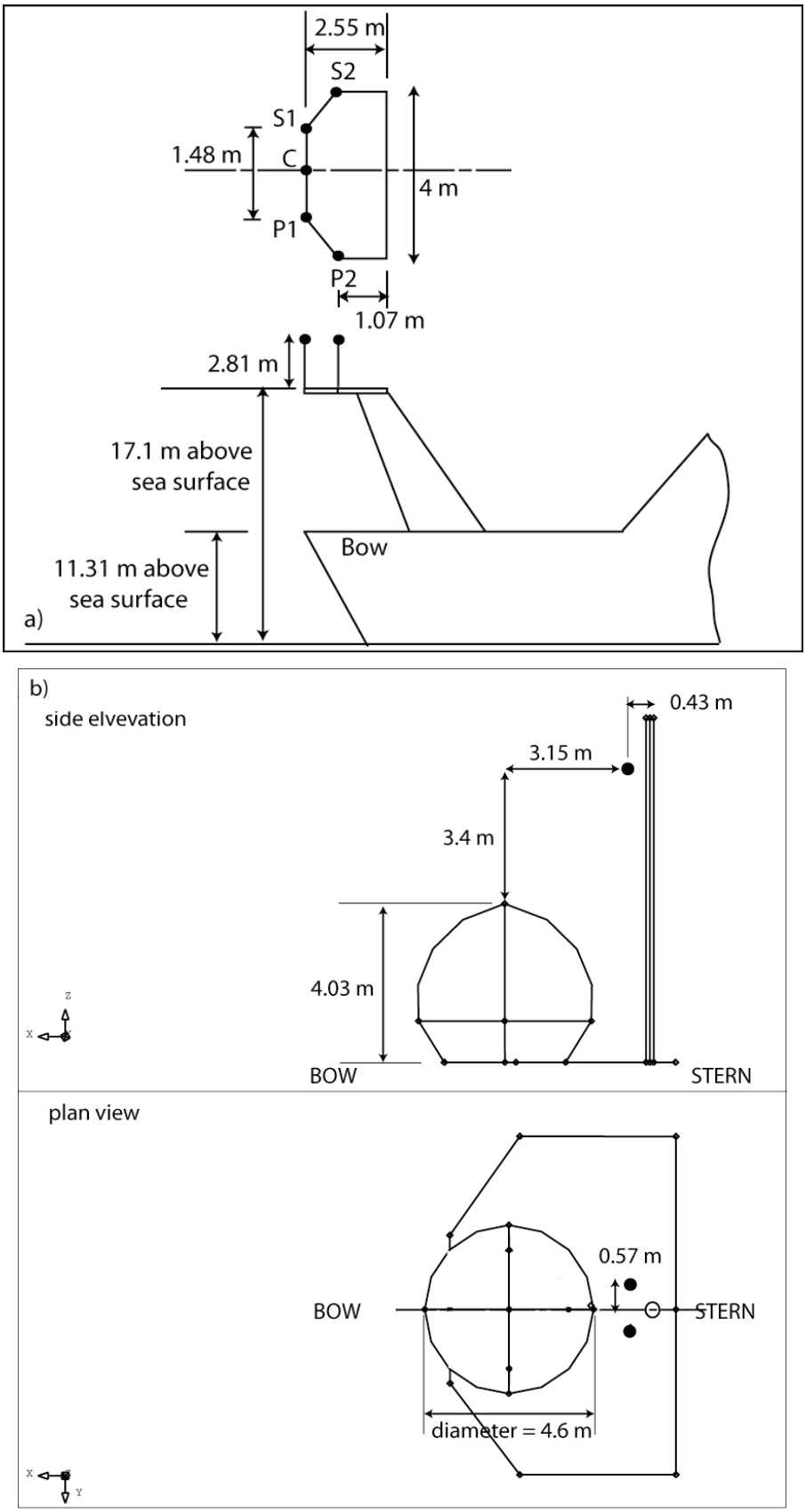

Figure 2 Schematic showing a) example instrument positions on the foremast, and b) the ship's anemometer positions relative to the main mast and the satellite communication radome.

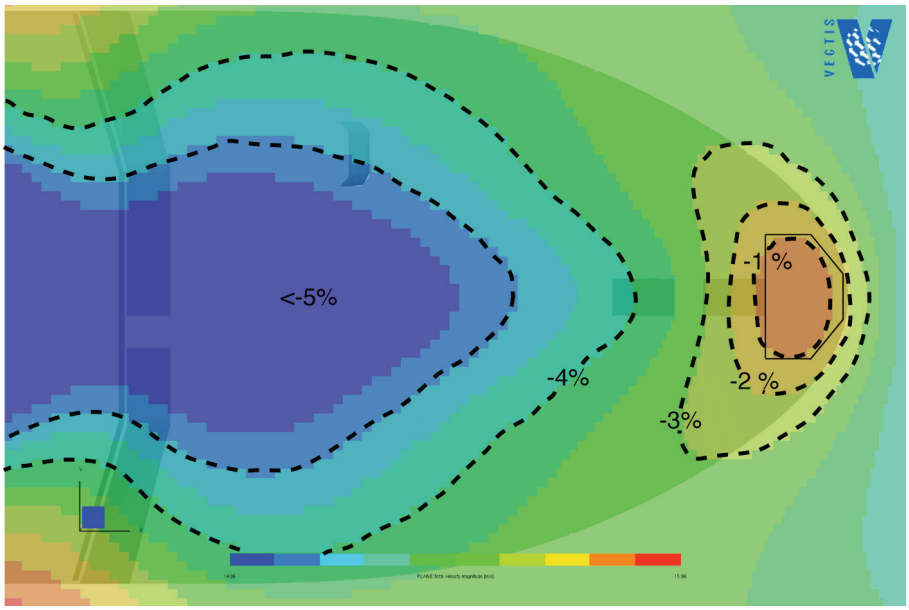

Figure 3 CFD model results for the airflow directly over the bow (0°) of the RRS *James Cook*. Data on a horizontal plane corresponding to the example anemometer height of 2.8 m above the platform (19.9 m above the sea surface) are shown. The contours indicate the wind speed bias expressed as a percentage of the free stream wind speed. A negative bias means a decelerated flow. The foremast platform is represented by the thin solid line and the underlying ship geometry is visible as darker shading.

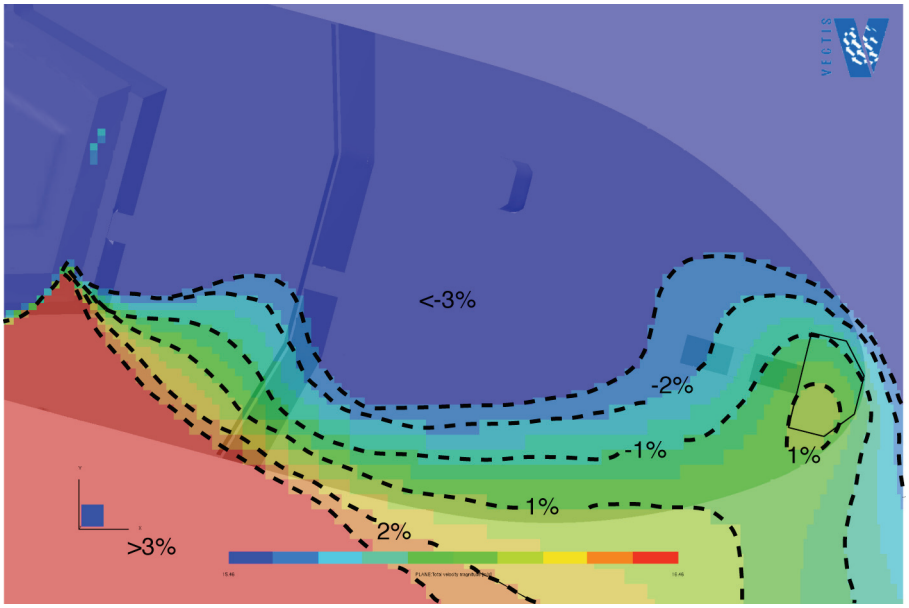

Figure 4 As Figure 3, but for a relative wind direction of 15° off the port bow. Note the change in colour scale.

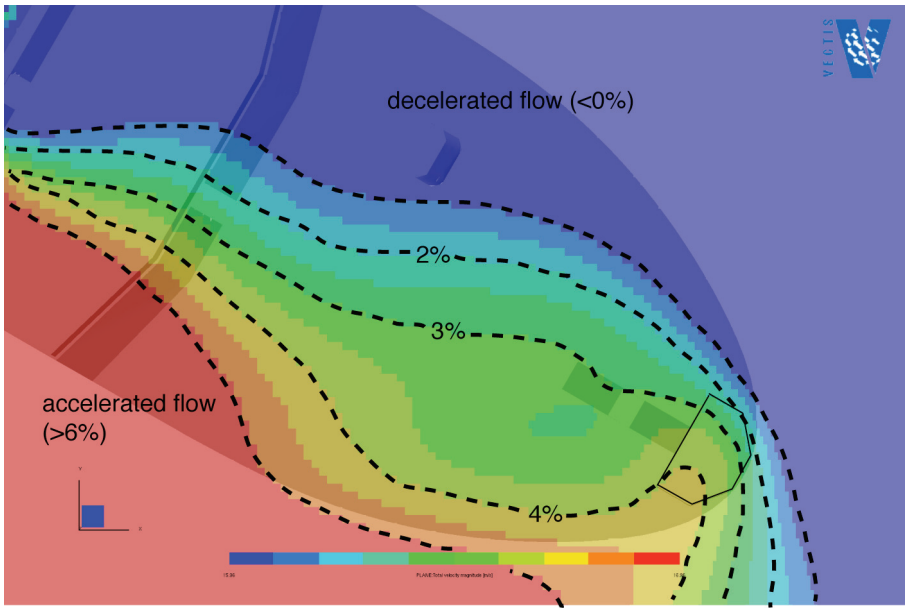

Figure 5 As Figure 3, but for a relative wind direction of 30° off the port bow. Note the change in colour scale.

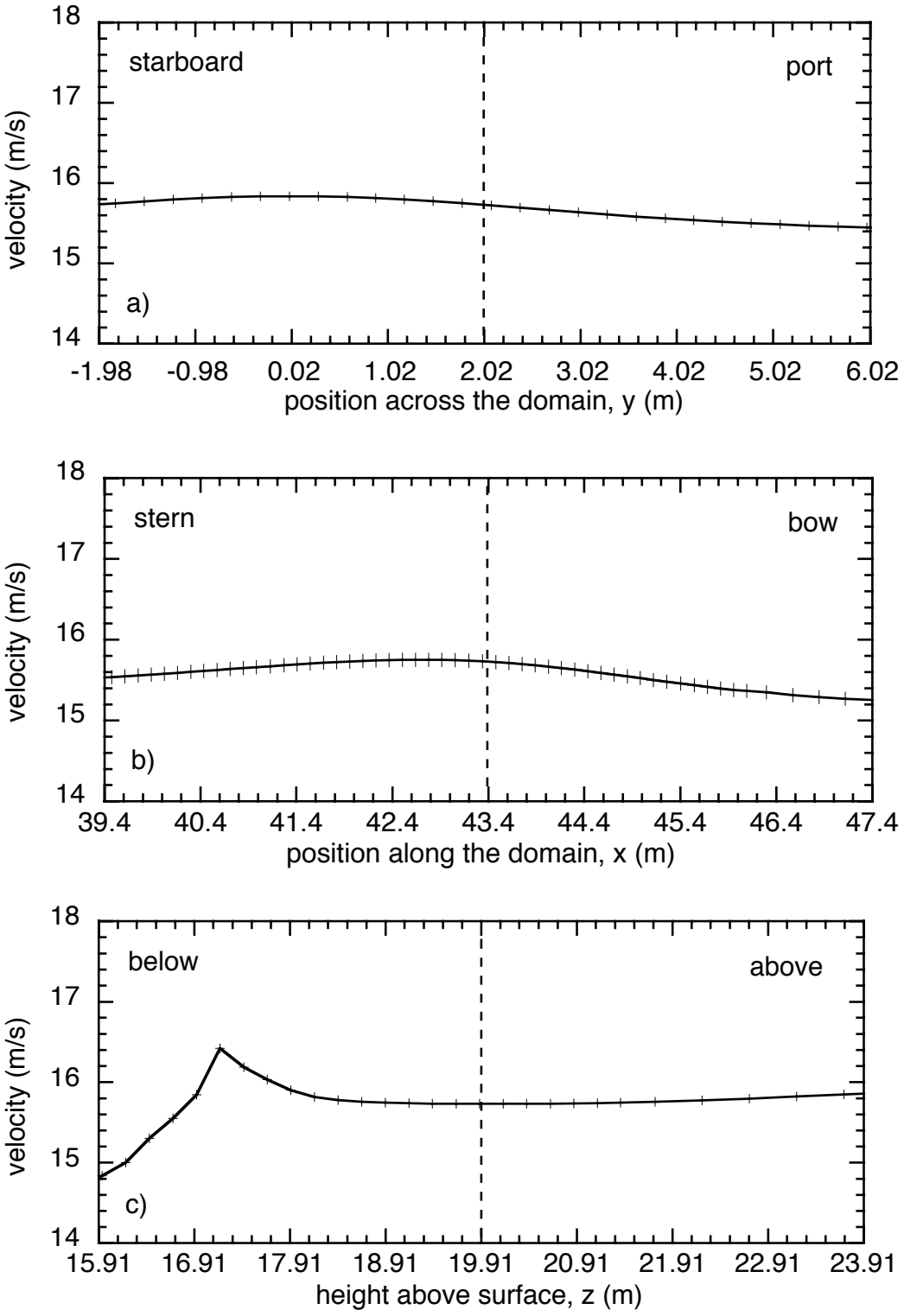

Figure 6 Lines of velocity data through the P2 anemometer position (indicated by the dashed line) in all three directions; a) across the tunnel (y), b) along the tunnel (x) and c) vertically (z). Results are from a bow-on flow.

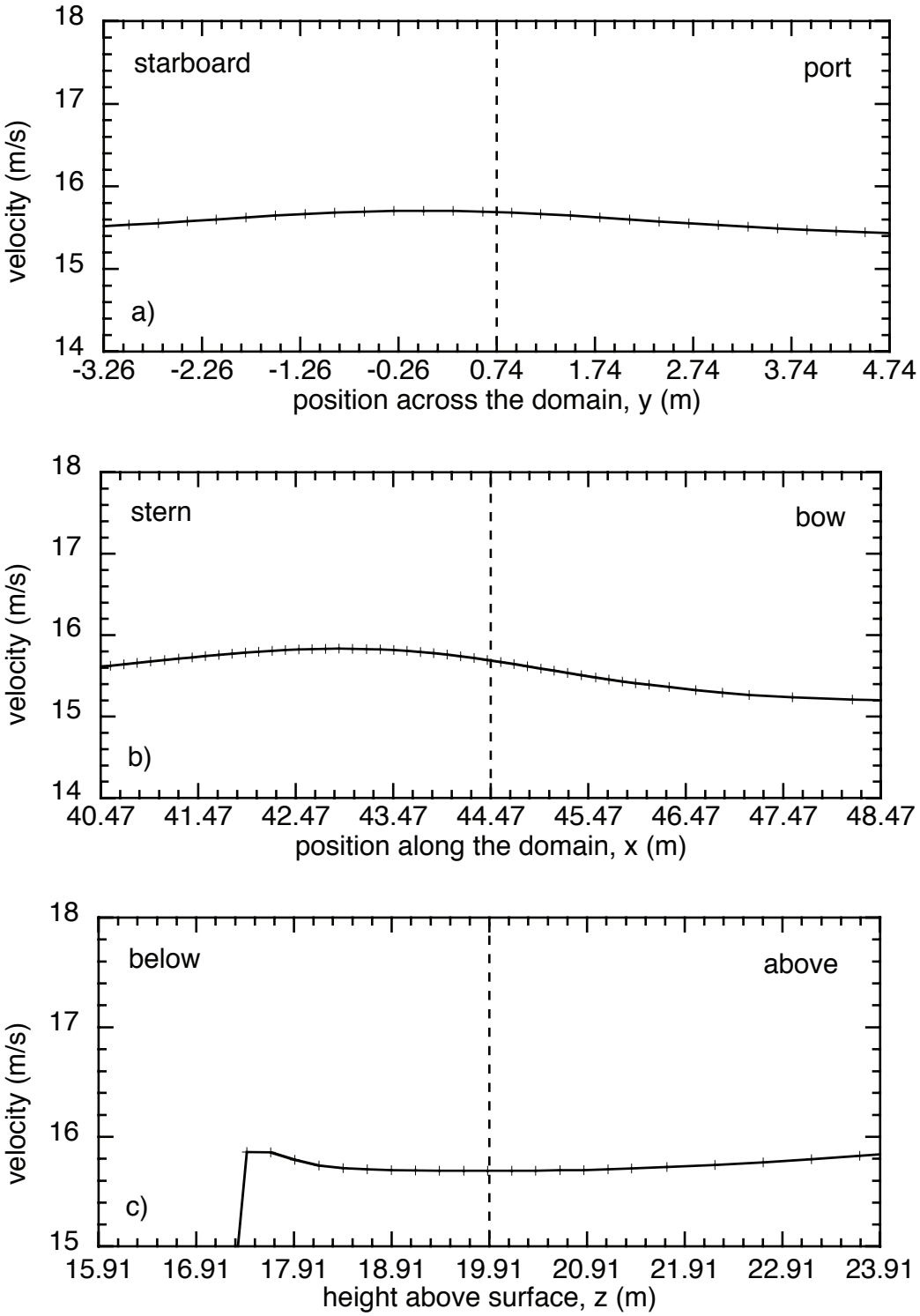

Figure 7 As for Figure 6, but for the P1 anemometer position. Results are from a bow-on flow.

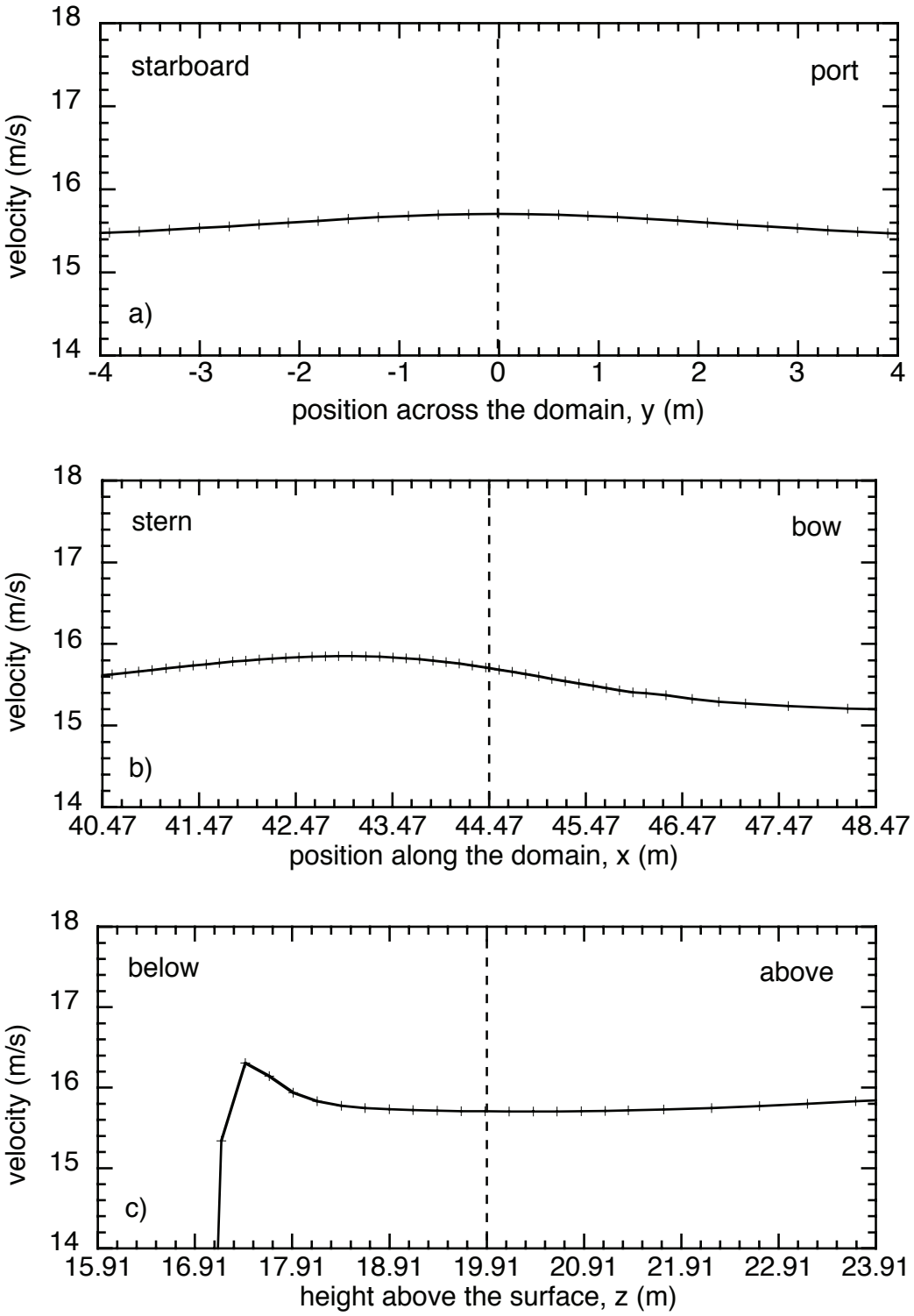

Figure 8 As for Figure 6, but for the C anemometer position. Results are from a bow-on flow.

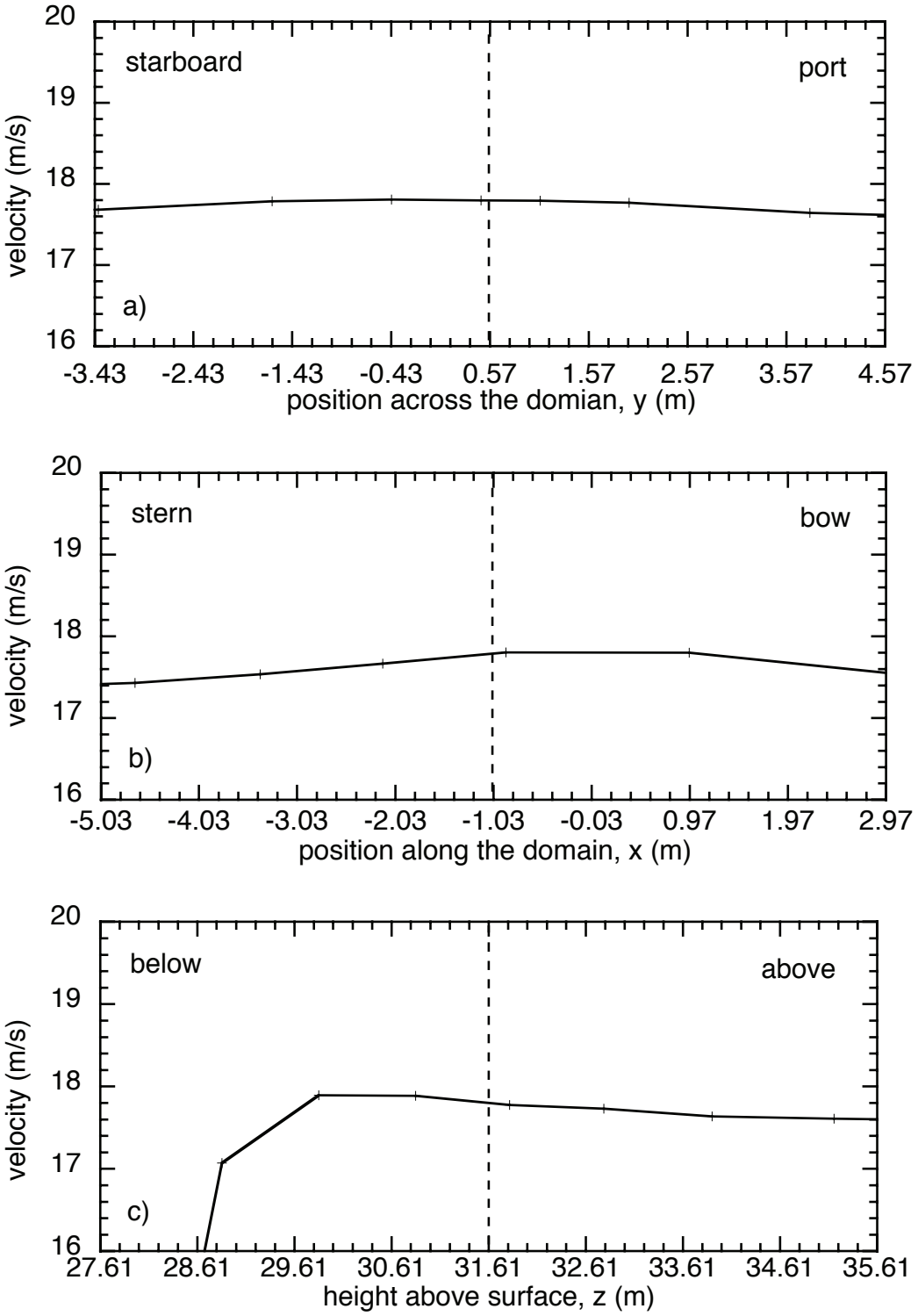

Figure 9 As for Figure 6, but for the port ships anemometer position. Results are from a bow-on flow.

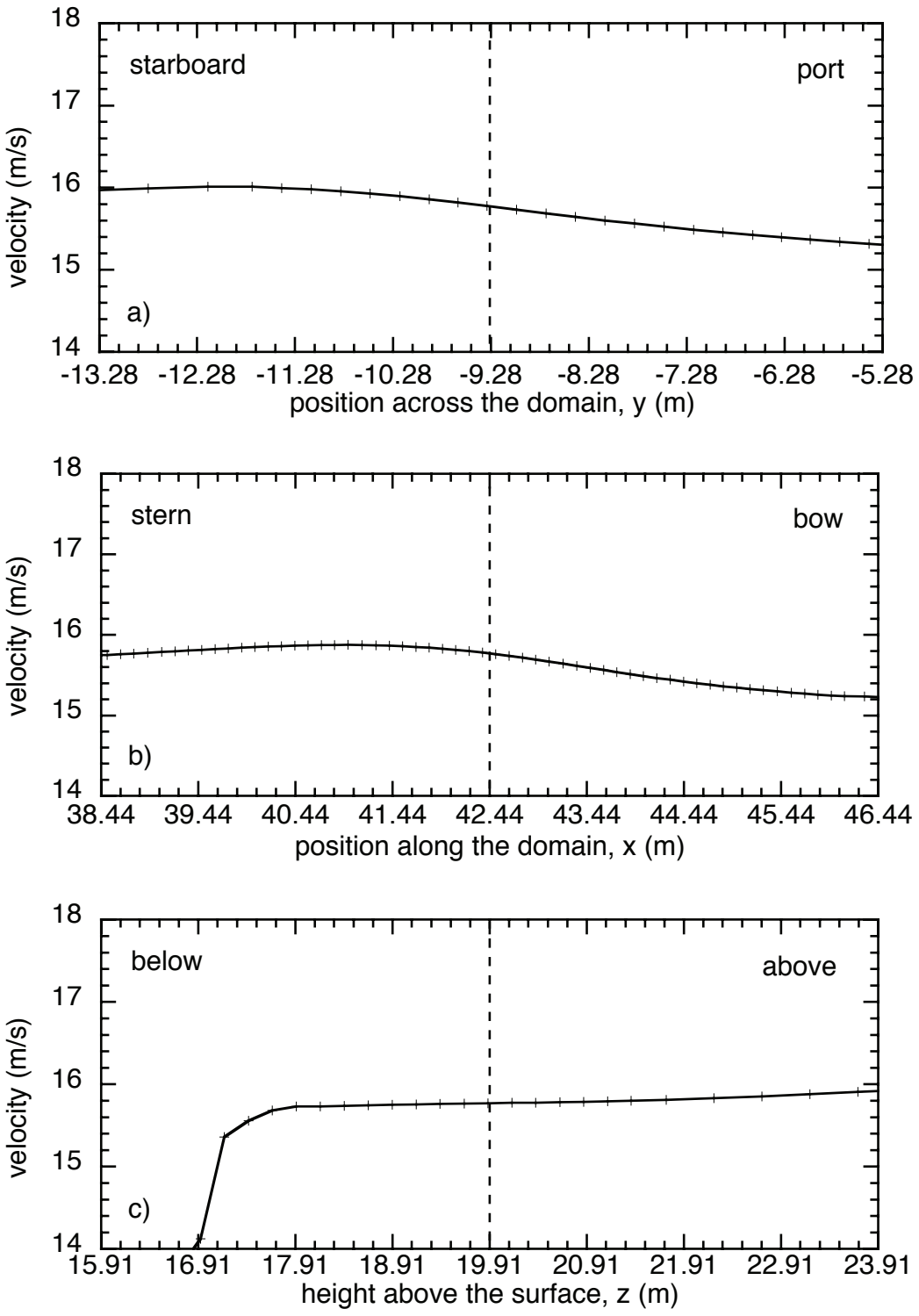

Figure 10 Lines of velocity data through the P2 anemometer position (indicated by the dashed line) in all three directions; a) across the tunnel (y), b) along the tunnel (x) and c) vertically (z). Results are from a flow 15° off the port bow.

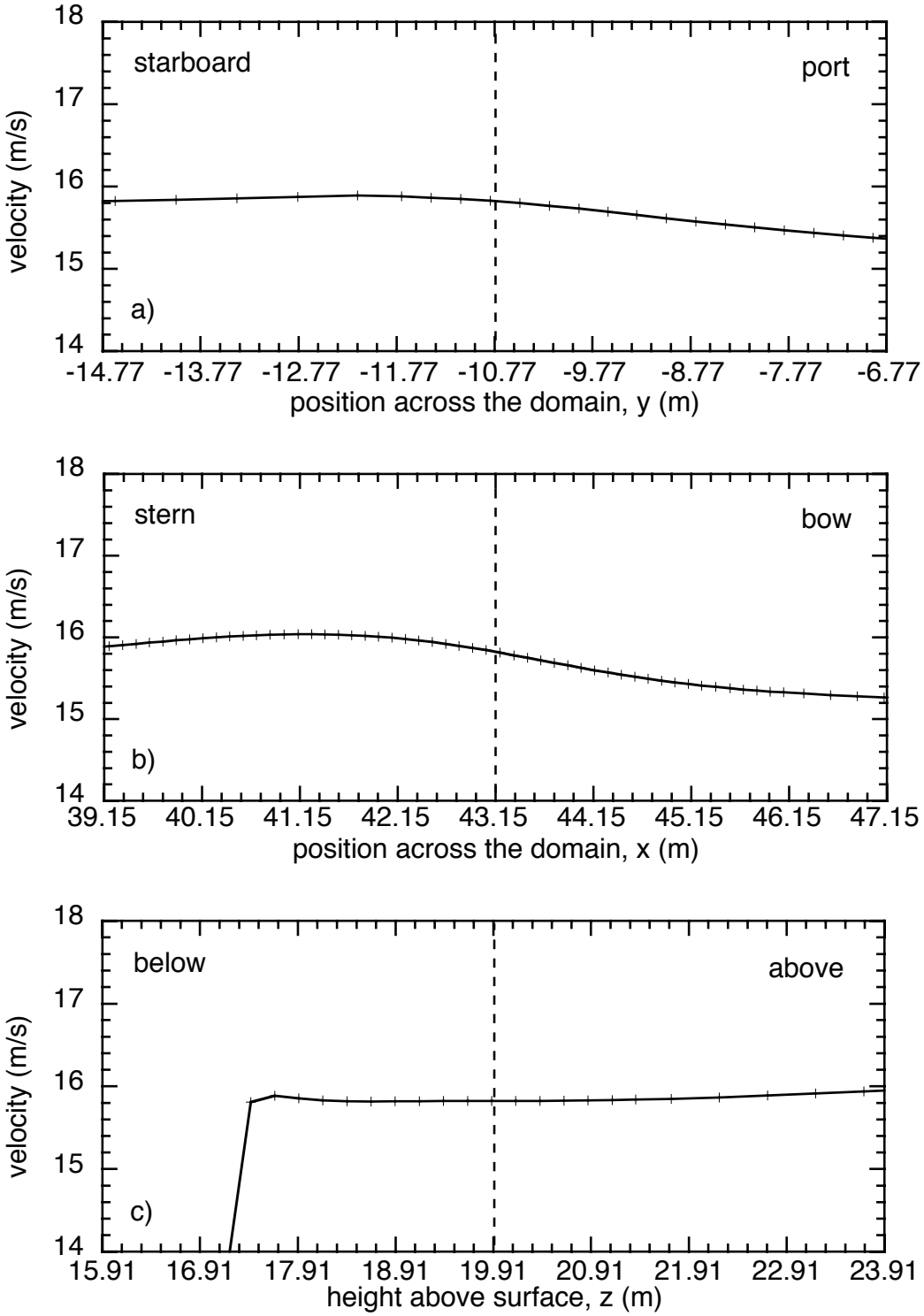

Figure 11 As for Figure 10, but for the P1 anemometer position. Results are from a flow 15° off the port bow.

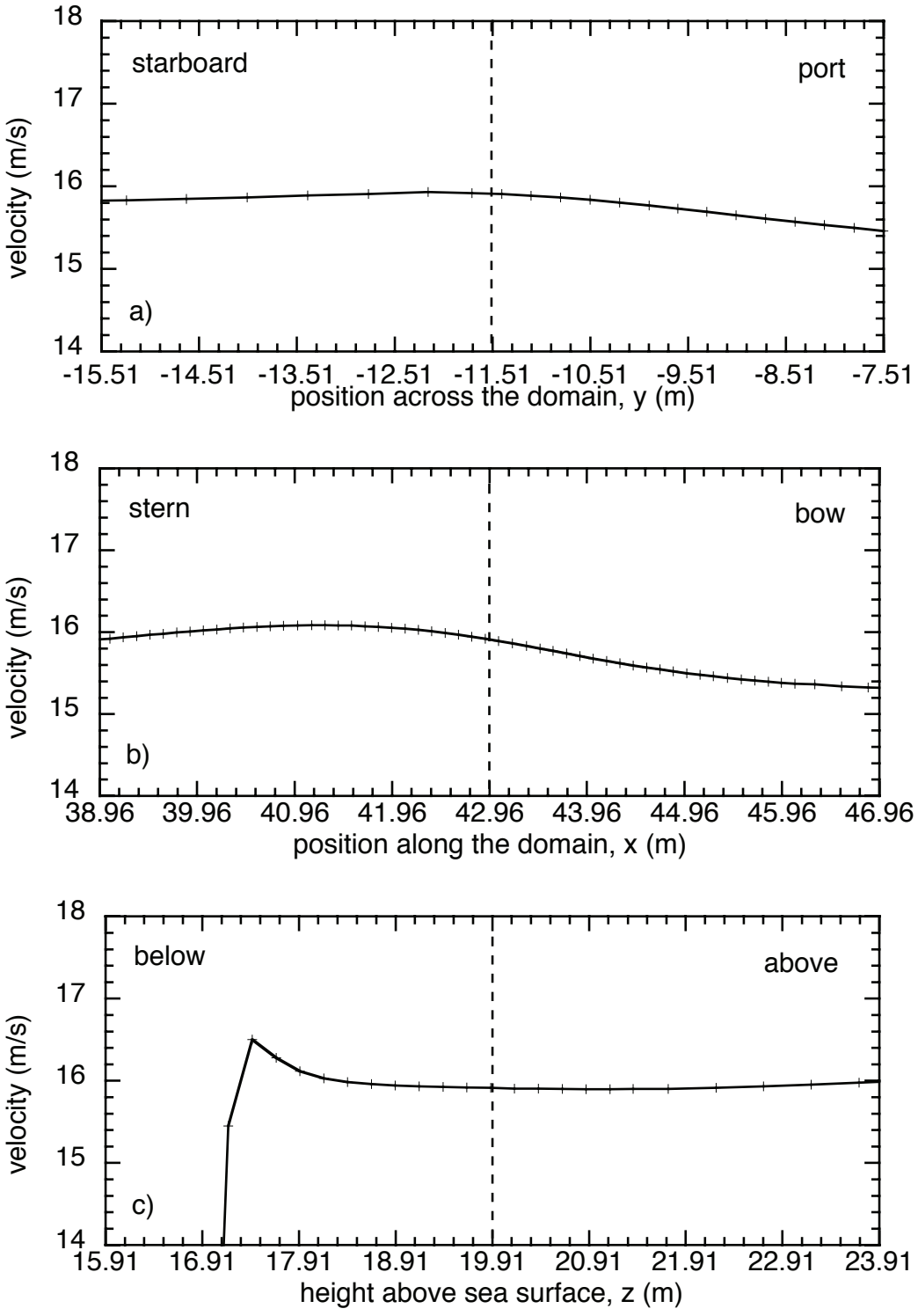

Figure 12 As for Figure 10, but for the C anemometer position. Results are from a flow 15° off the port bow.

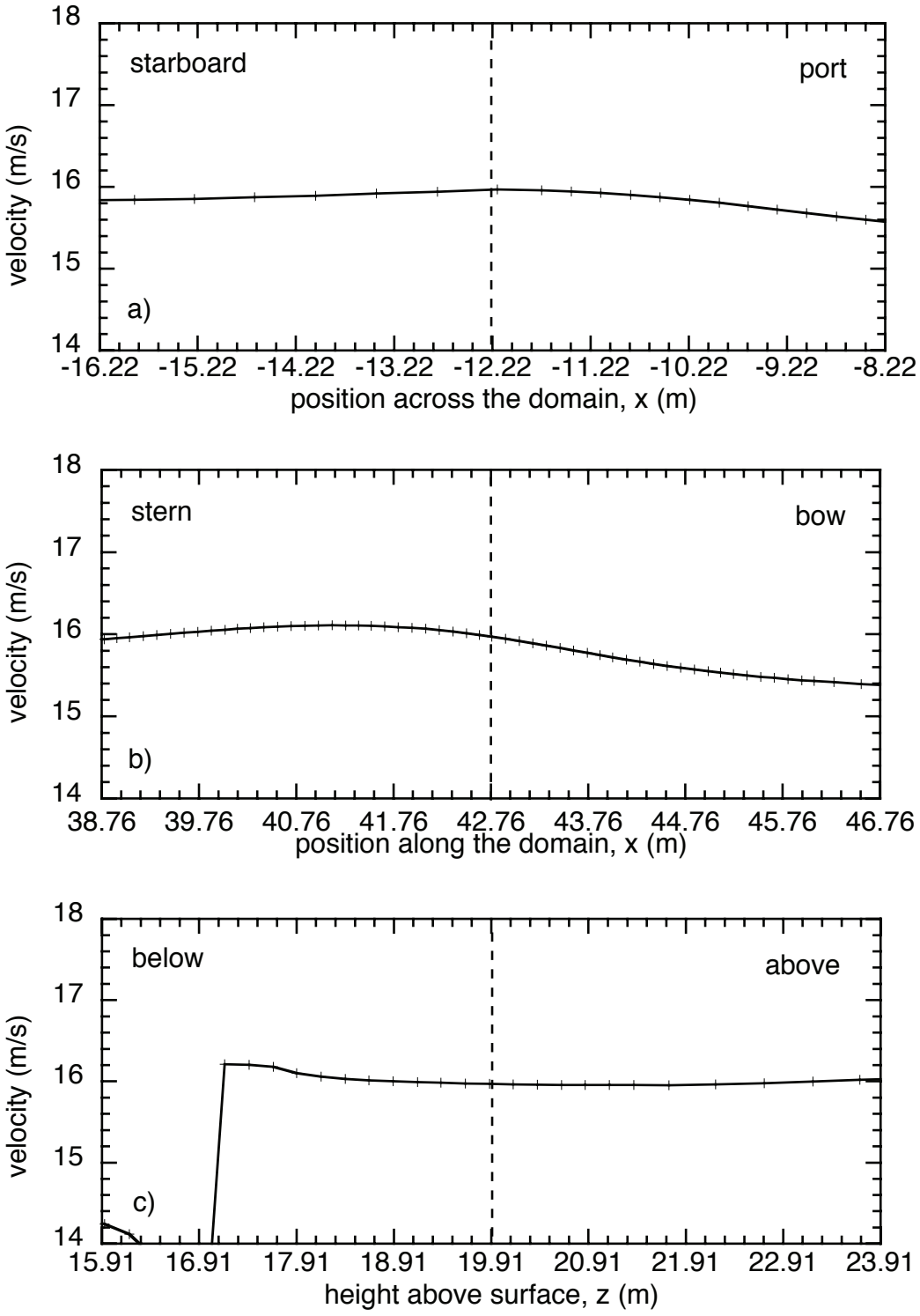

Figure 13 As for Figure 10, but for the S1 anemometer position. Results are from a flow 15° off the port bow.

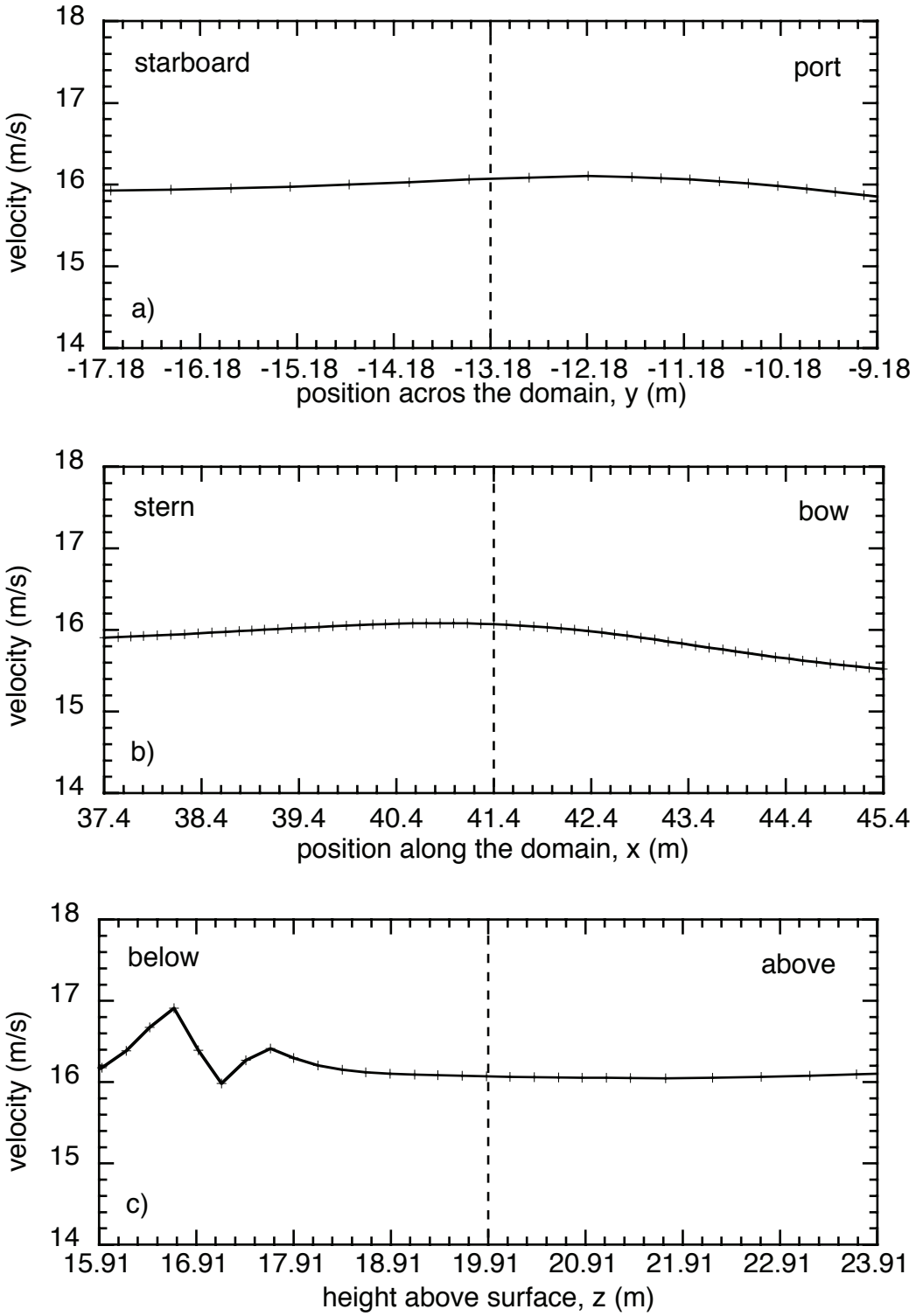

Figure 14 As for Figure 10, but for the S2 anemometer position. Results are from a flow 15° off the port bow.

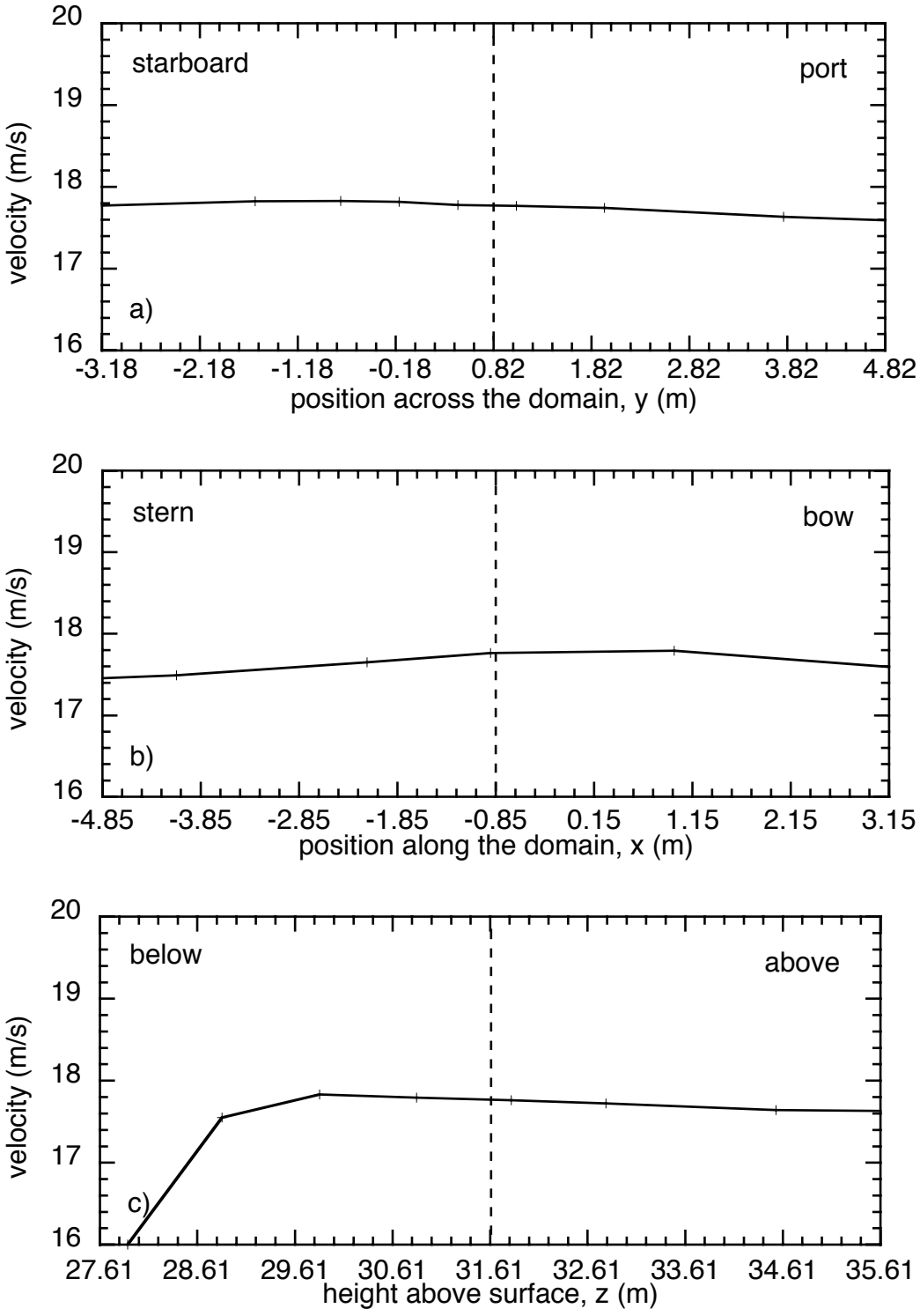

Figure 15 As for Figure 10, but for the port ship's anemometer position. Results are from a flow 15° off the port bow.

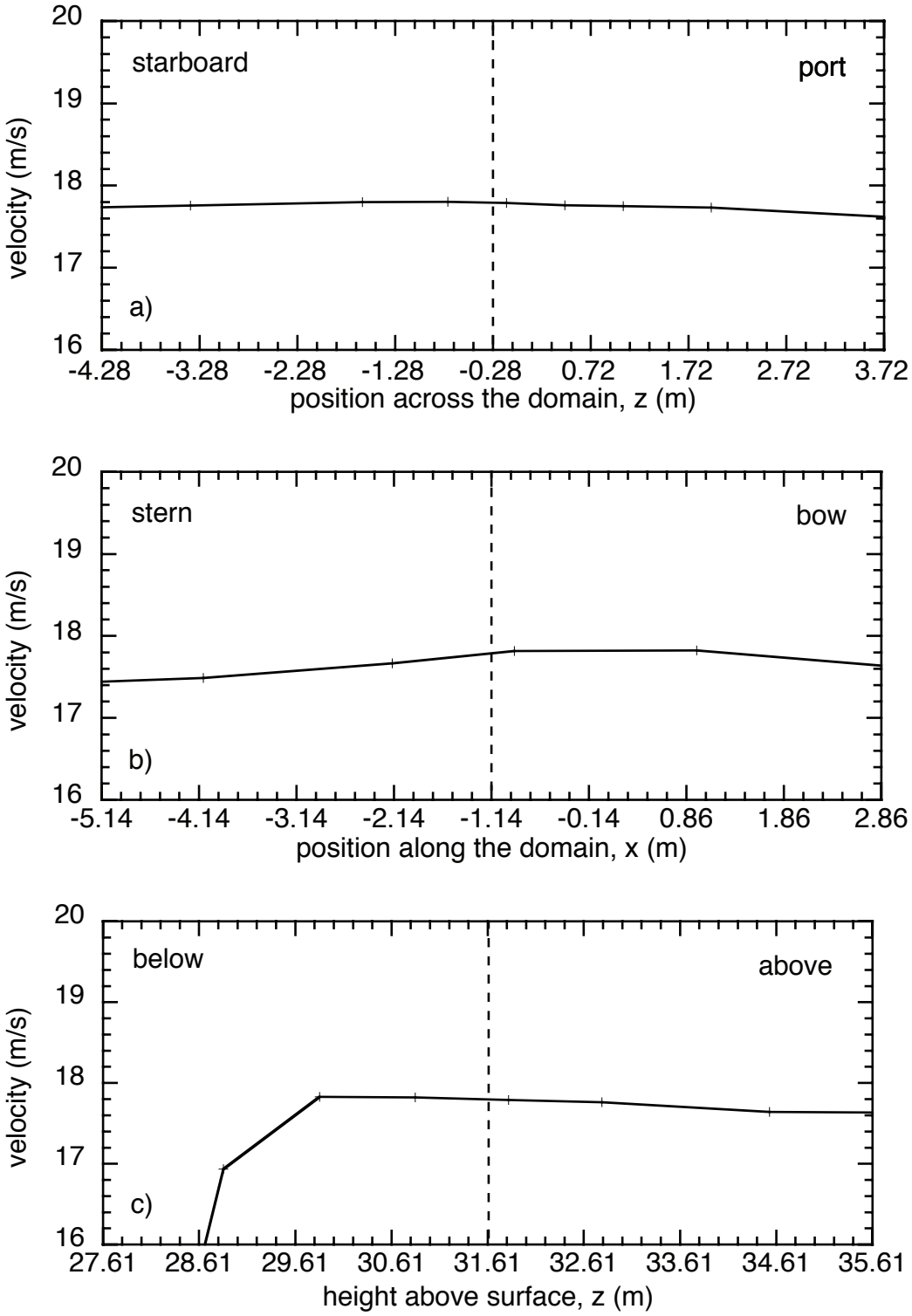

Figure 16 As for Figure 10, but for the starboard ship's anemometer position. Results are from a flow 15° off the port bow.

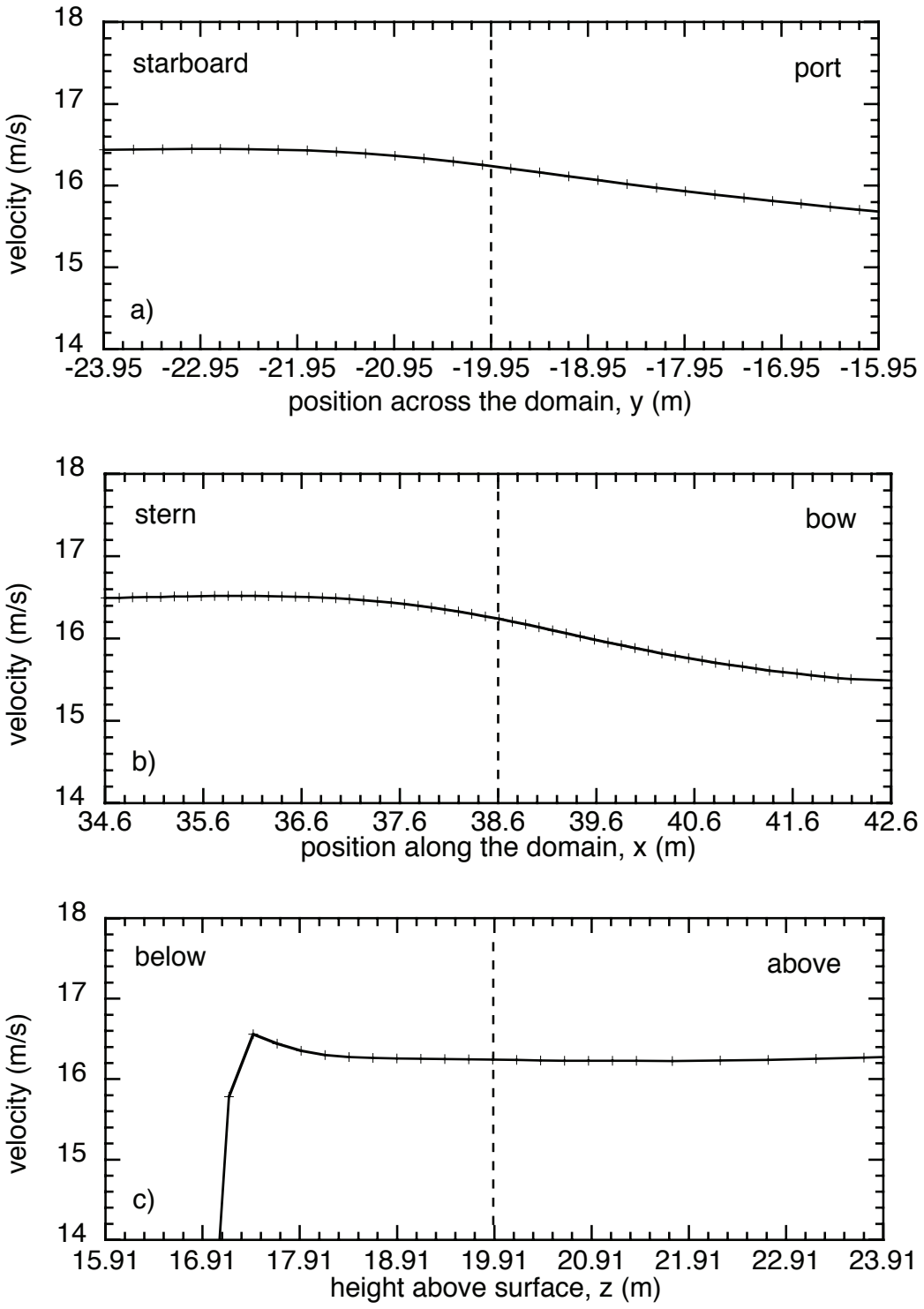

Figure 17 Lines of velocity data through the P2 anemometer position (indicated by the dashed line) in all three directions; a) across the tunnel (y), b) along the tunnel (x) and c) vertically (z). Results are from a flow 30° off the port bow.

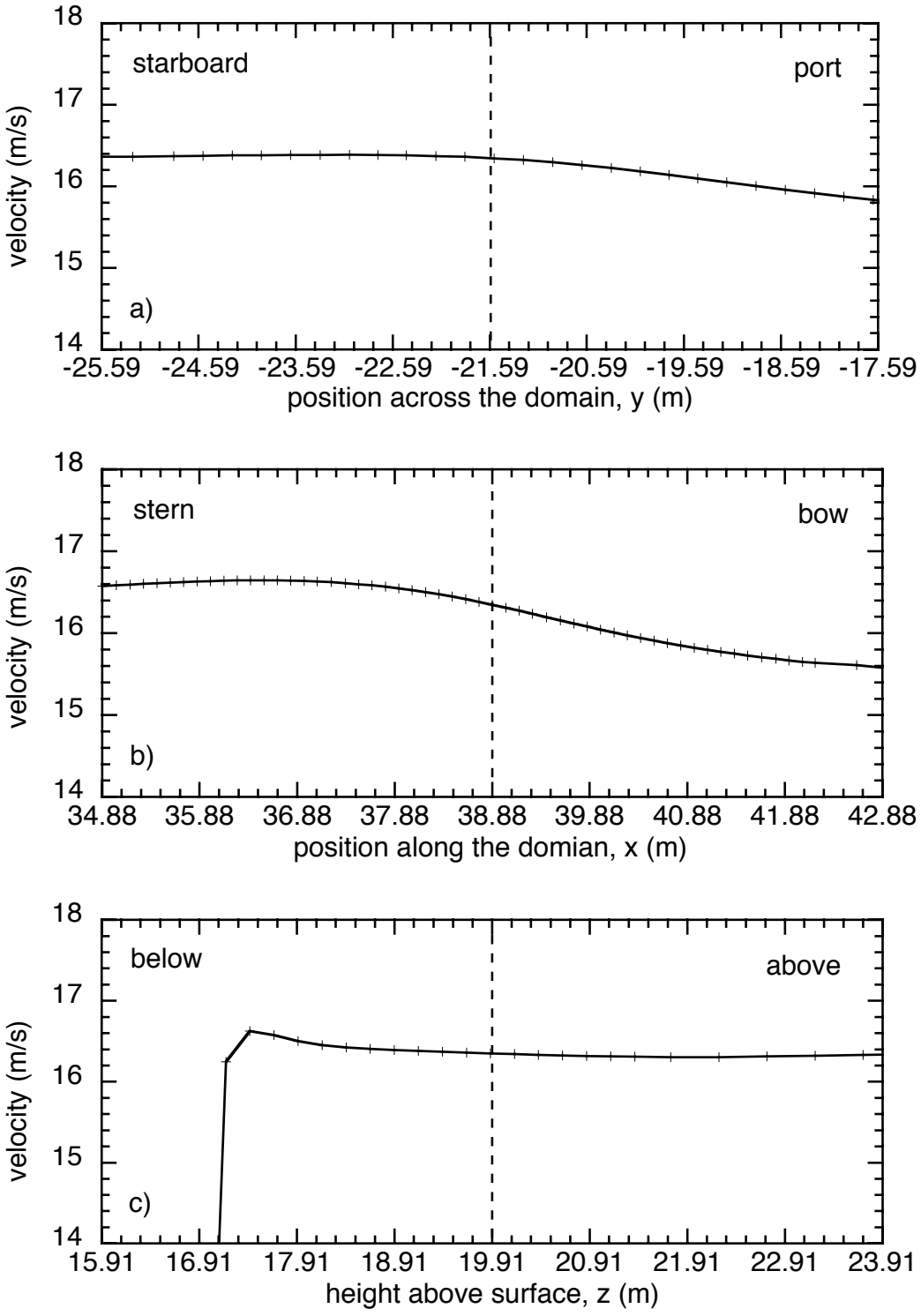

Figure 18 As for Figure 17, but for the P1 anemometer position. Results are from a flow 30° off the port bow.

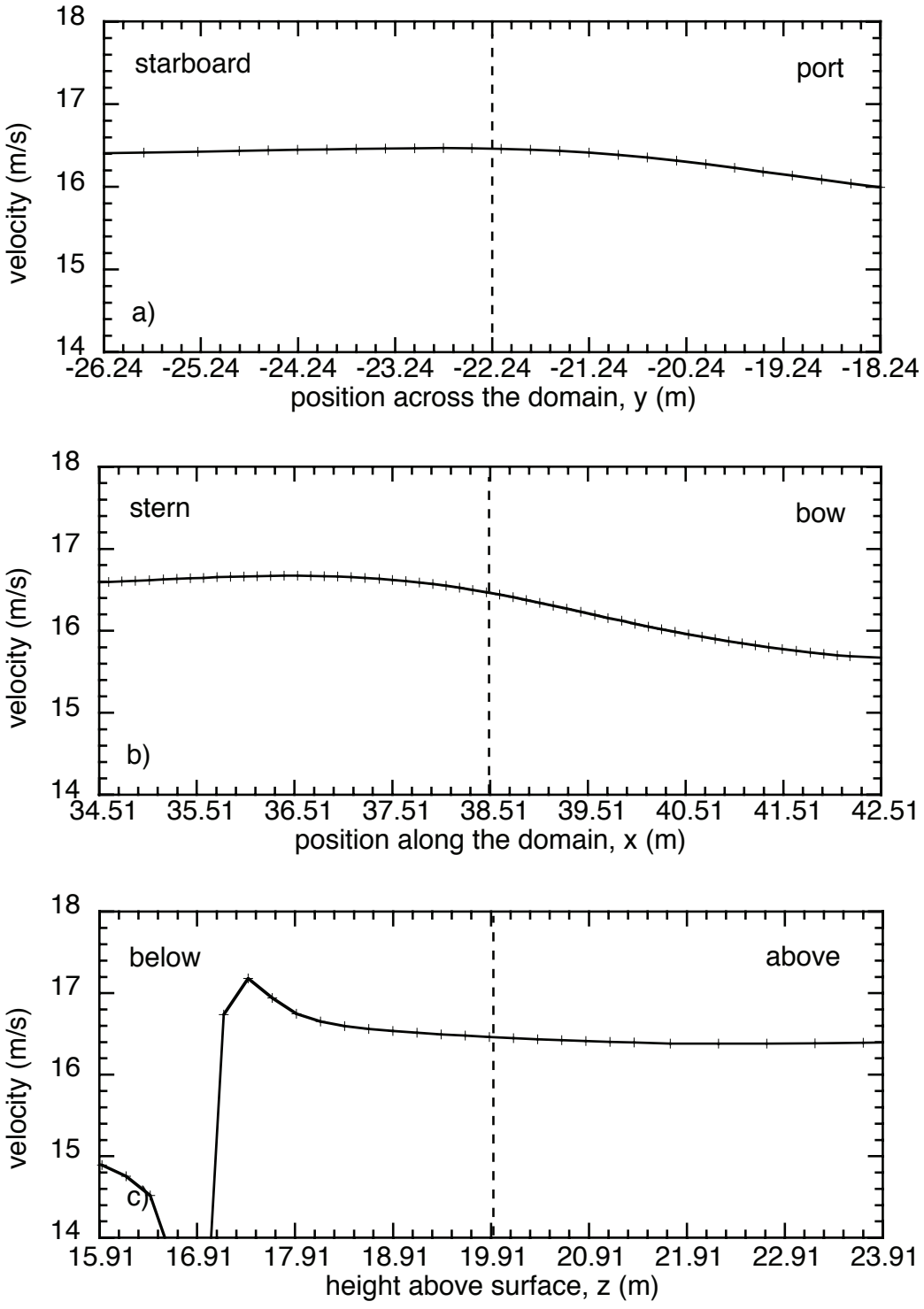

Figure 19 As for Figure 17, but for the C anemometer position. Results are from a flow 30° off the port bow.

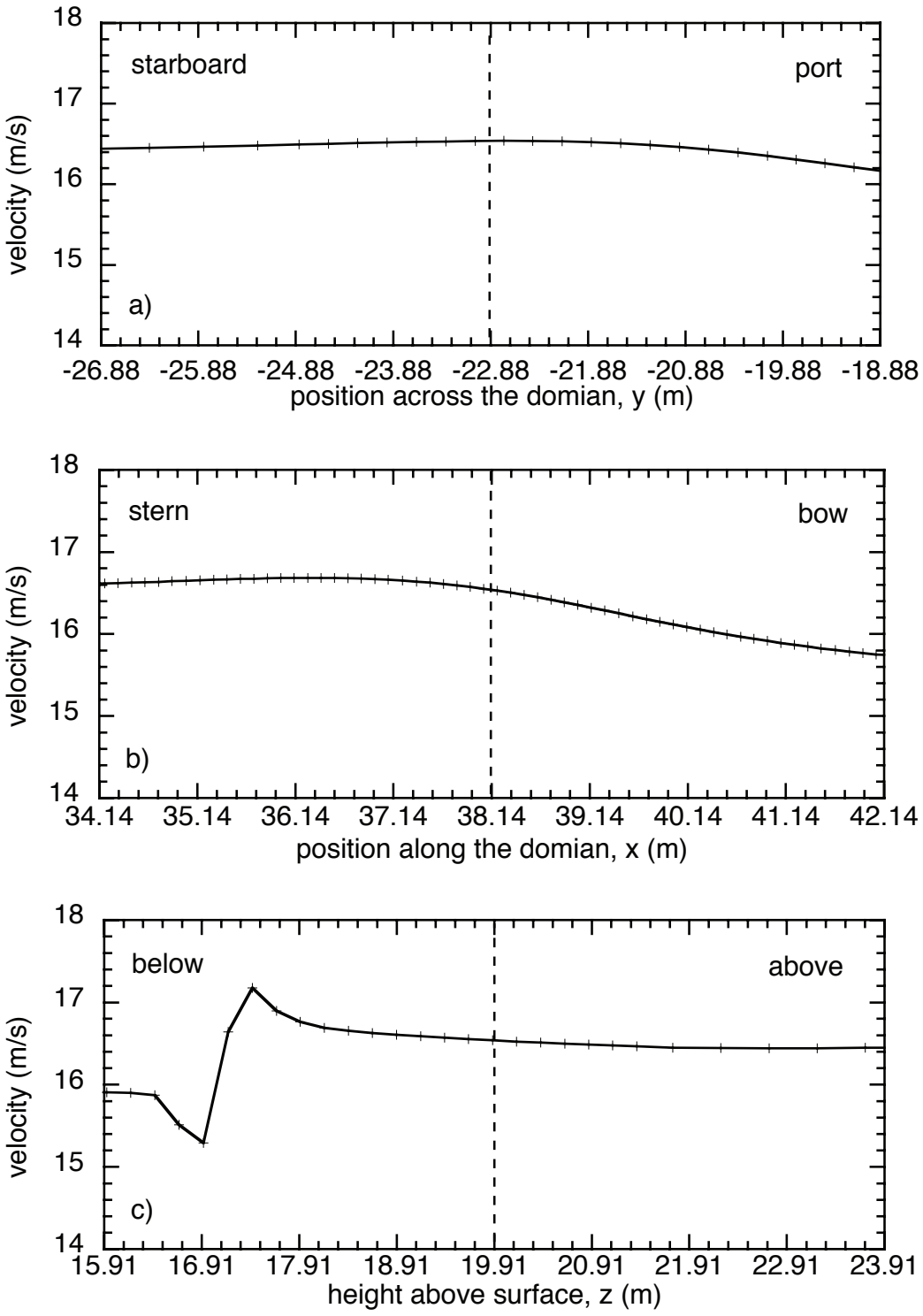

Figure 20 As for Figure 17, but for the S1 anemometer position. Results are from a flow 30° off the port bow.

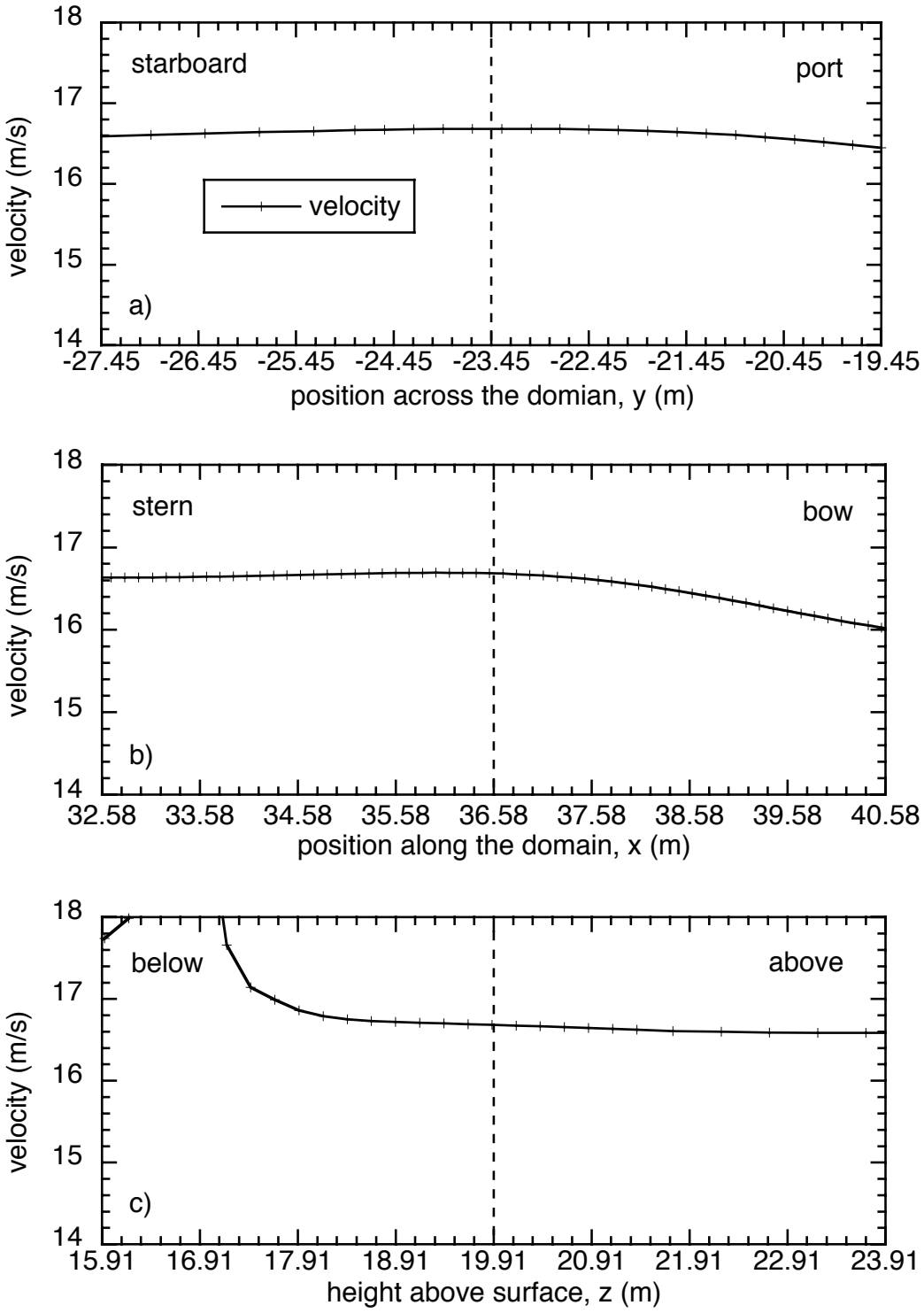

Figure 21 As for Figure 17, but for the S2 anemometer position. Results are from a flow 30° off the port bow.

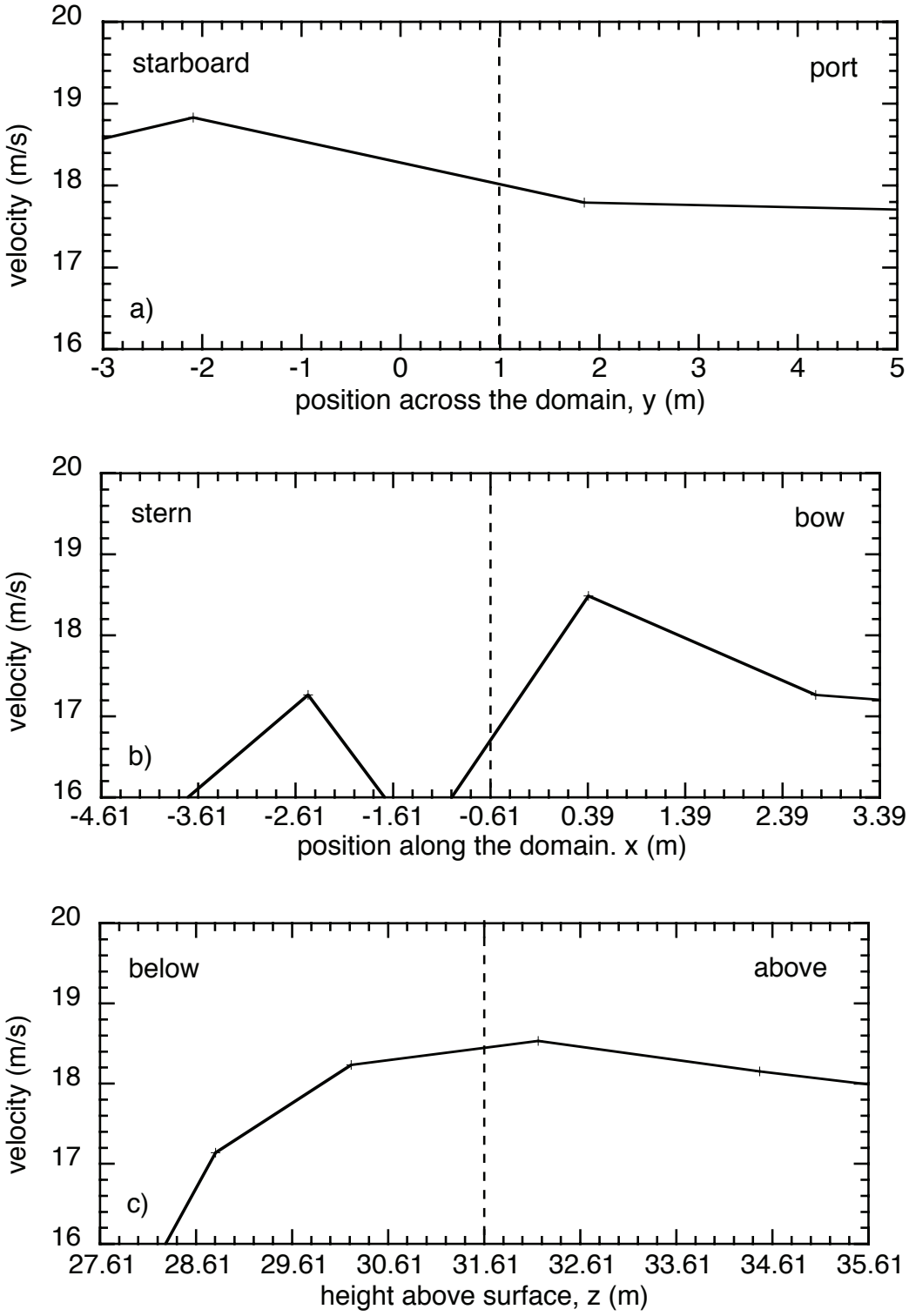

Figure 22 As for Figure 17, but for the port ship's anemometer position. Results are from a flow 30° off the port bow.

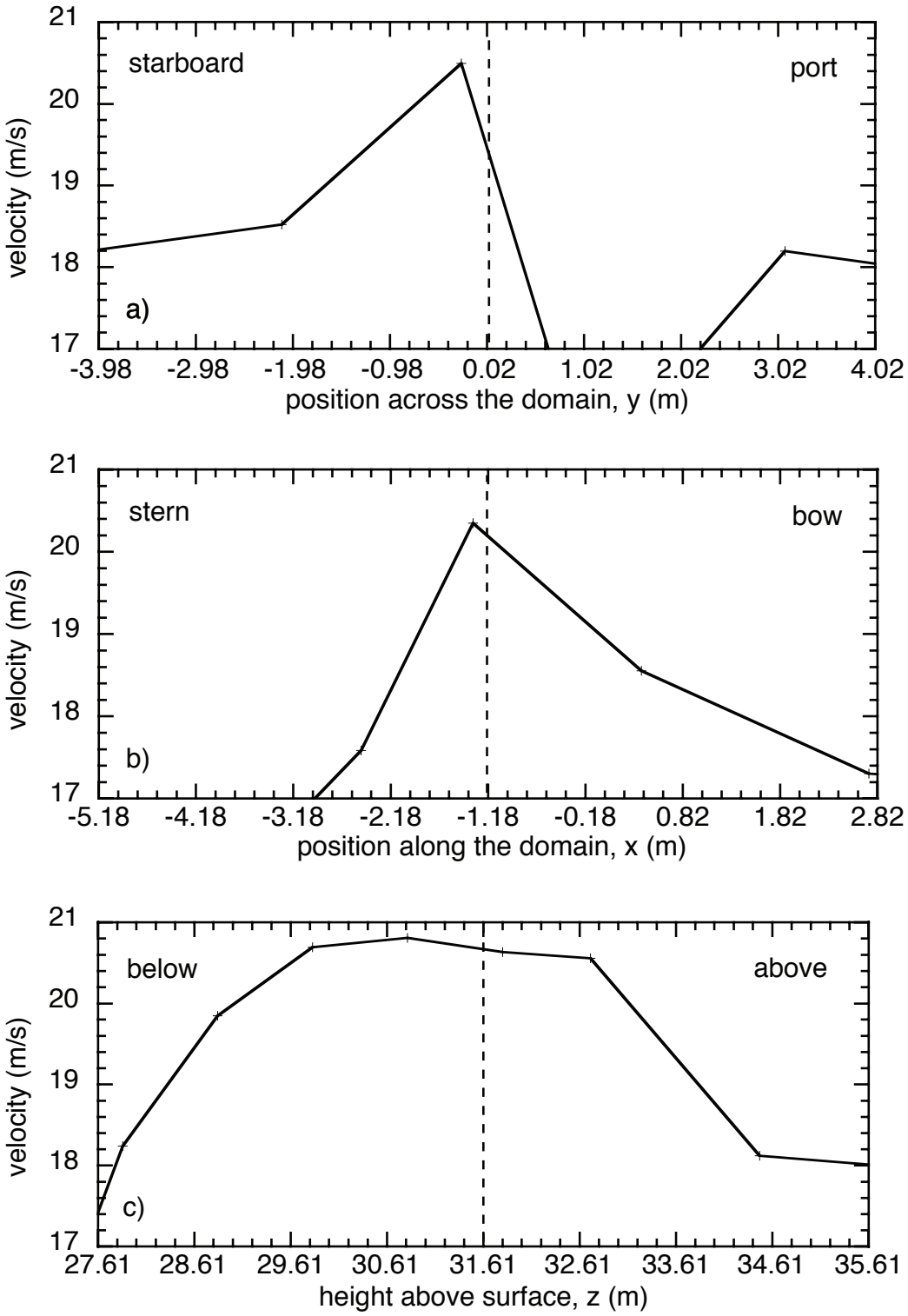

Figure 23 As for Figure 17, but for the starboard ship's anemometer position. Results are from a flow 30° off the port bow.

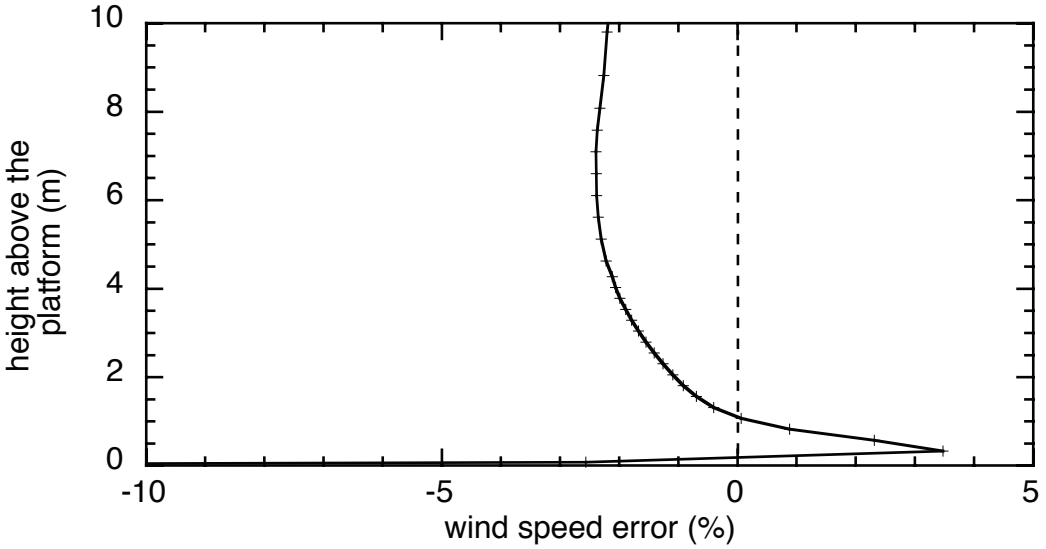

Figure 24 Vertical profile of the wind speed error obtained through ‘C’ foremast anemometer location for a bow-on flow.

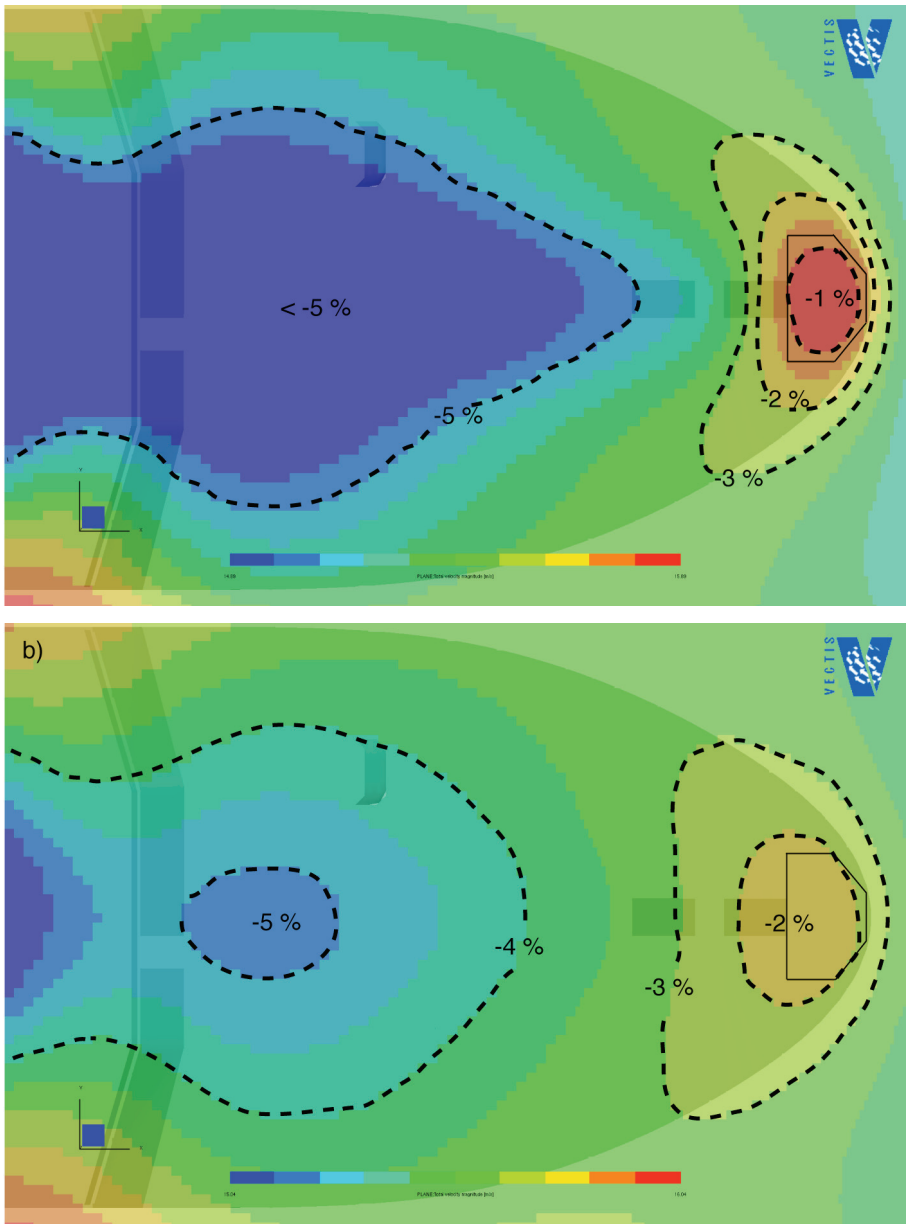

Figure 25 CFD model results for the airflow directly over the bow (0°) of the RRS *James Cook*. Only data on a horizontal plane corresponding to the typical anemometer height of a) 2 m and b) 4 m above the platform are shown. The contours indicate the wind speed bias (i.e. the measured wind speed as a percentage of the free stream wind speed). A negative bias means a decelerated flow. The foremast platform is represented by the thin solid line and the underlying ship geometry is visible as darker shading.

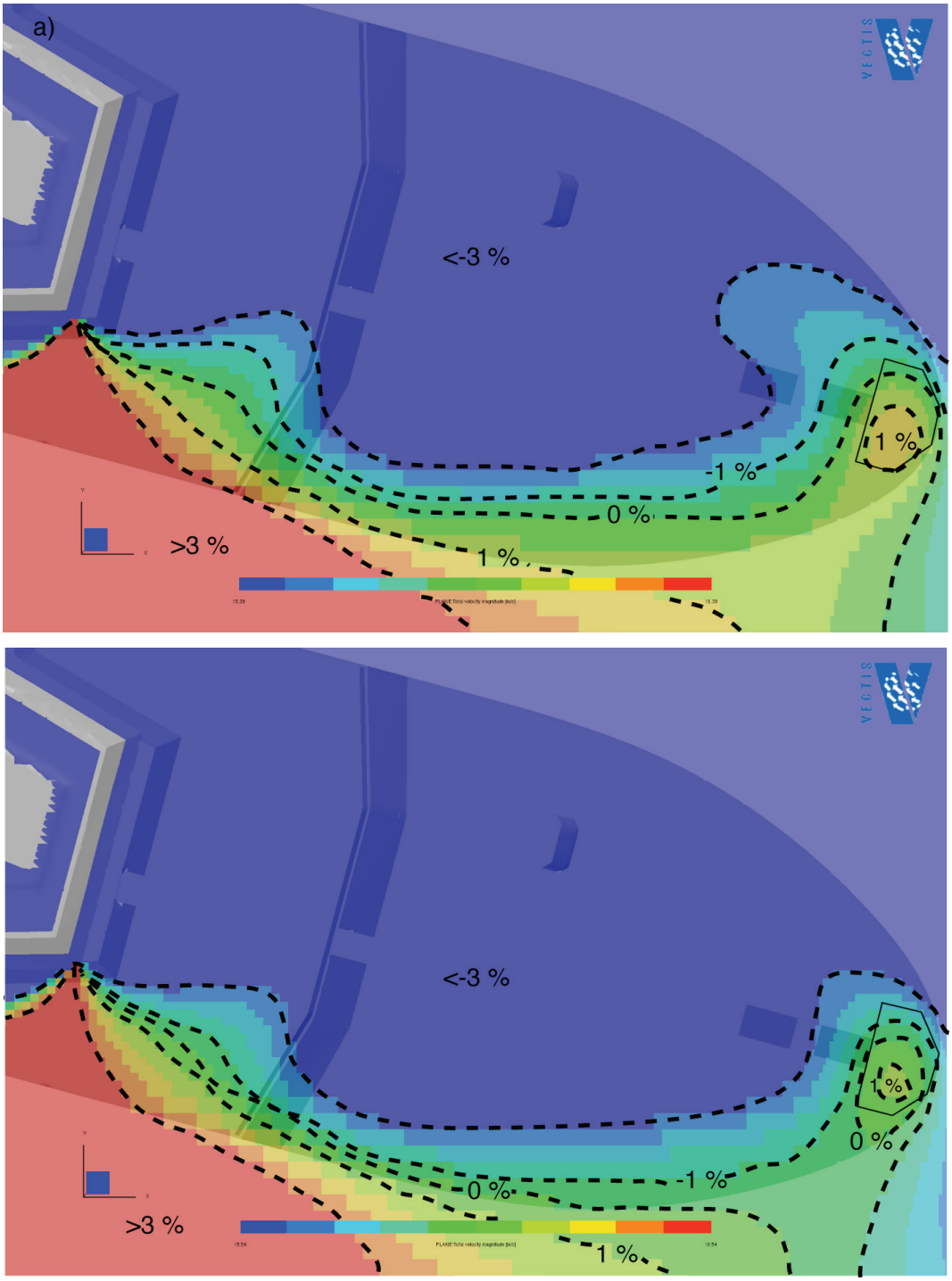

Figure 26 As Figure 25, but for a relative wind direction of 15° off the port bow. Note the change in colour scale.

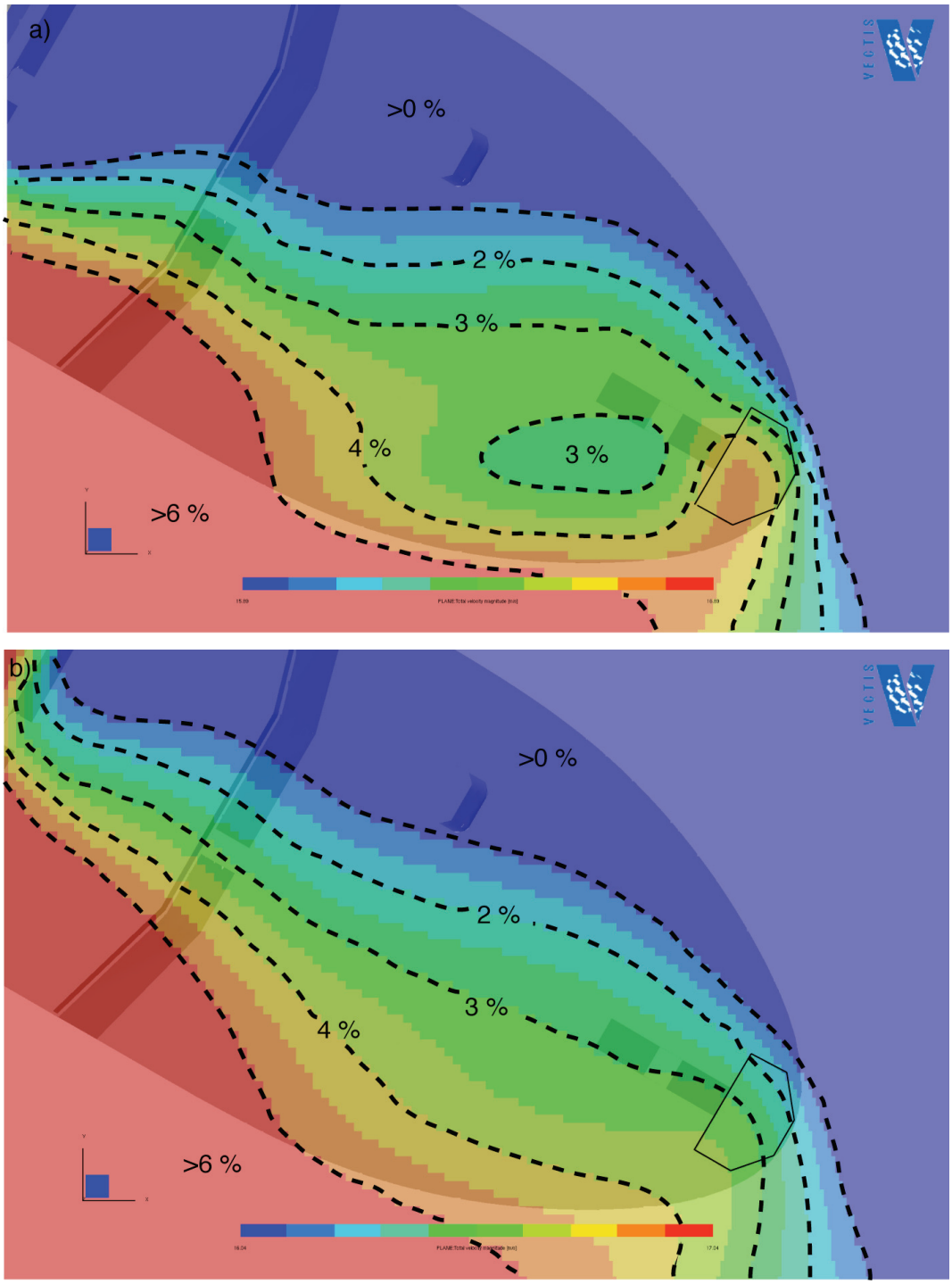

Figure 27 As Figure 25, but for a relative wind direction 30° off the port bow. Note the change in colour scale.

APPENDIX

The Figures in this appendix were generated using the VECTIS post-processing software. The variable size of the computational domain can be seen in all the Figures.

FIGURE A1 – Velocity vectors on a vertical plane through the C anemometer located on the front edge of the foremast platform. The position of the starboard side ships anemometer is shown. The airflow is directly over the bow and the magnitude of the total velocity in indicated by the colour of the arrows.

FIGURE A2 – As Figure A1, but for a relative wind direction of 15° off the port bow.

FIGURE A3 – As Figure A1, but for a relative wind direction of 30° off the port bow.

FIGURE A4 – Velocity vectors on a vertical plane through the starboard ship's anemometer position located on the main mast for a relative wind direction of 30° off the port bow.

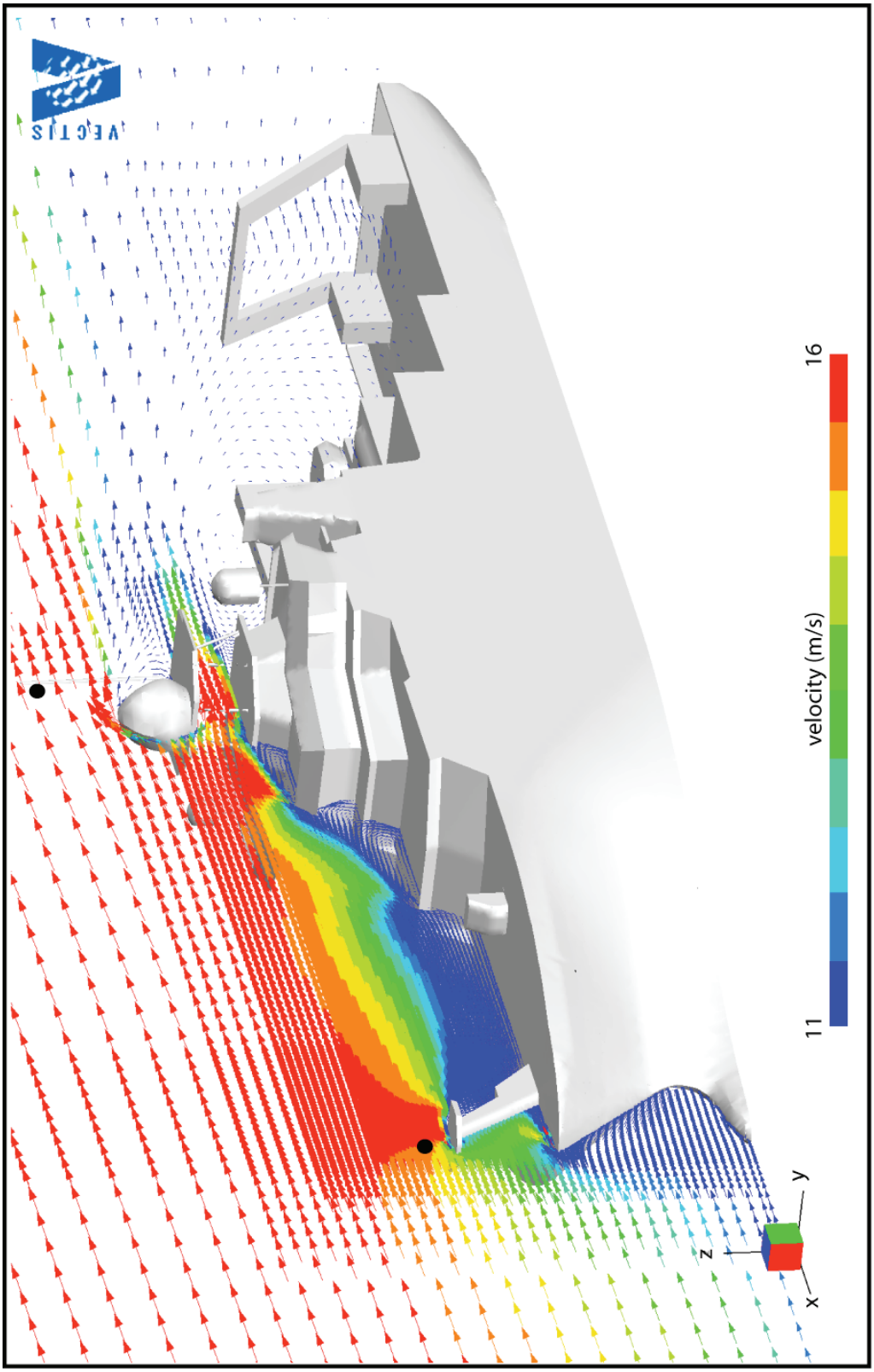

Figure A1

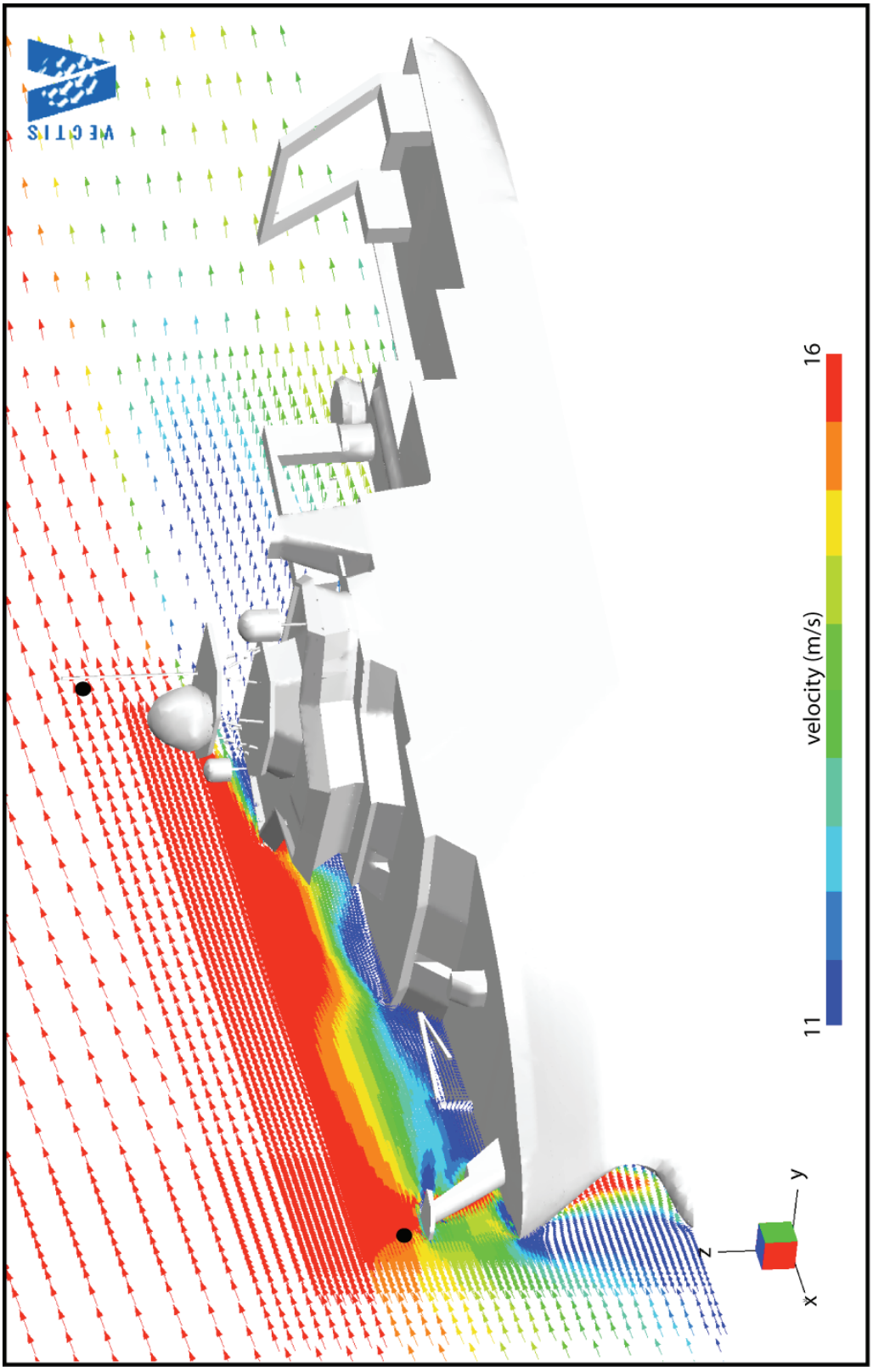

Figure A2

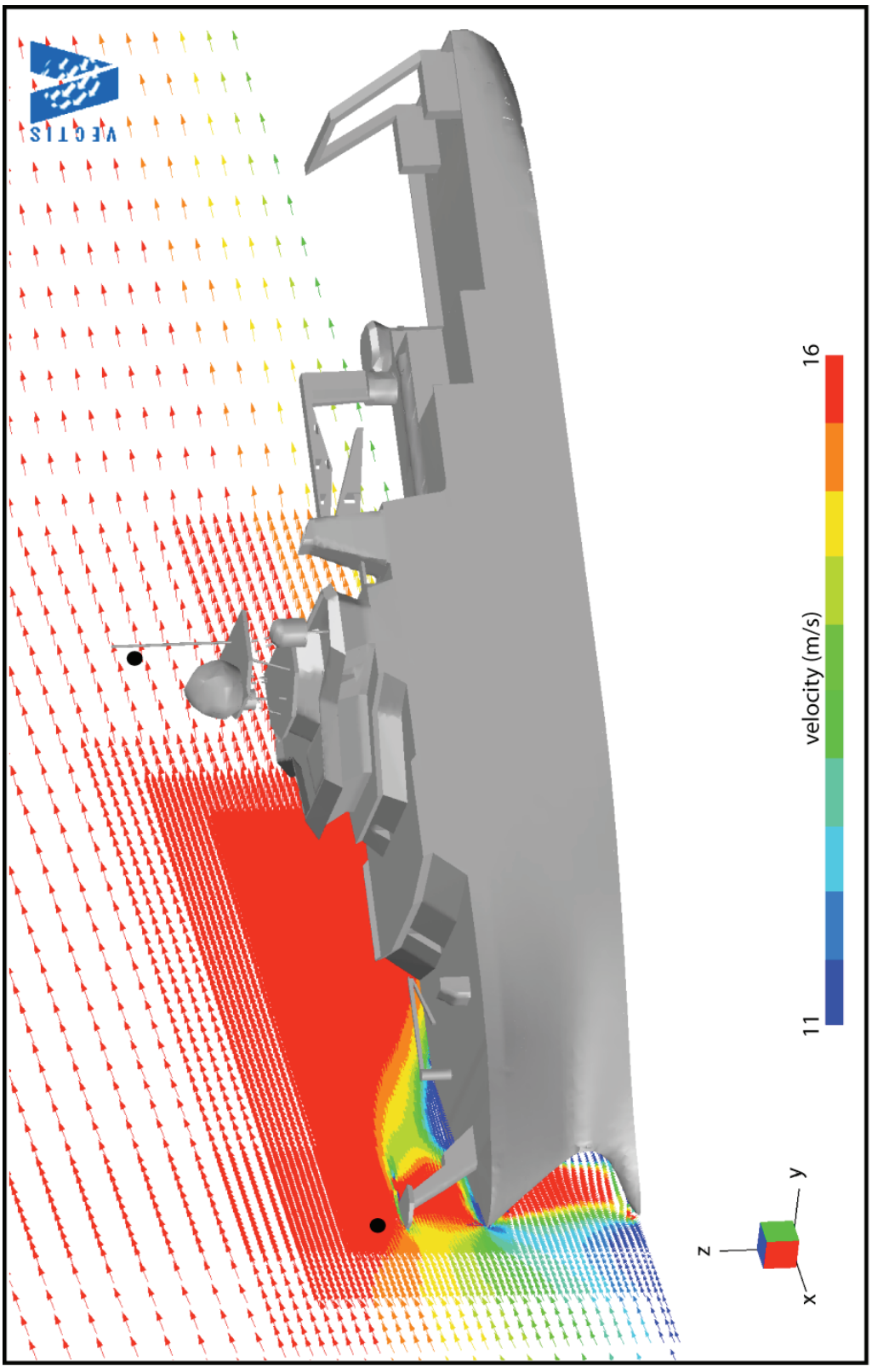

Figure A3

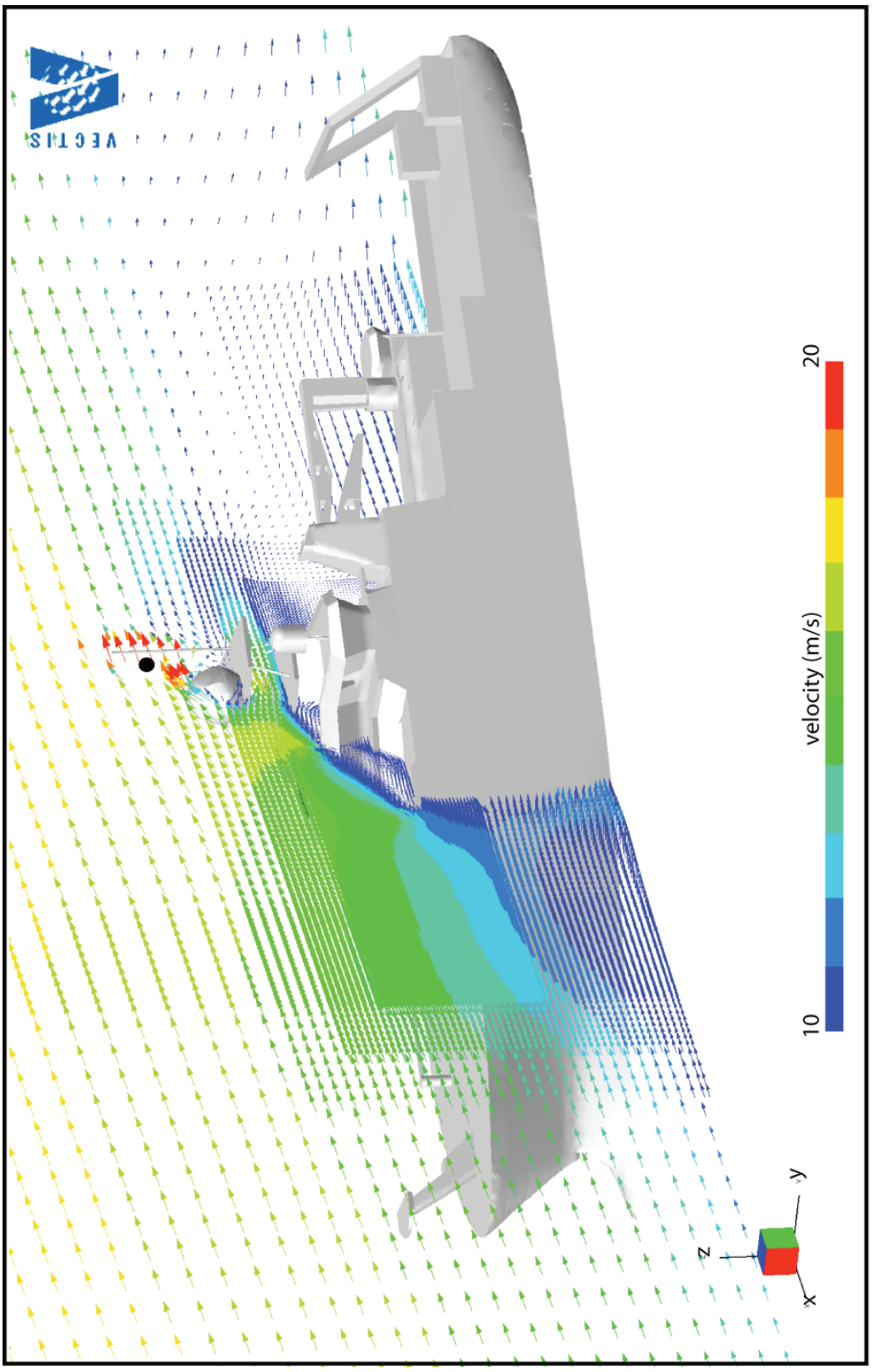

Figure A4